Identification of soluble bone loss biomarkers in cystic fibrosis patients

Sofia de Araújo Ribeiro Pinto Ferreira
Master´s Degree in Cell and Molecular Biology
Biology Department
Faculty of Sciences of the University of Porto
2023/2024

Identification of soluble bone loss biomarkers in cystic fibrosis patients

Sofia de Araújo Ribeiro Pinto Ferreira

Dissertation carried out as part of the Master's degree in Cell and Molecular Biology

Biology Department

2023/2024

Supervisor
Dina Cosme, Post-doctoral Fellow, Instituto de Investigação e Inovação em Saúde (i3S), University of Porto

Co-supervisors
Ana Cordeiro Gomes, Project Principal Investigator, Instituto de Investigação e Inovação em Saúde (i3S) Universidade do Porto, Medical Resident, Unidade Saúde Local São João

Salomé Gomes, Group leader, Instituto de Investigação e Inovação em Saúde (i3S); Full Professor, Instituto de Ciências Biomédicas de Abel Salazar (ICBAS), Universidade do Porto

Dedicated to my friends and family

Agradecimentos

Ao terminar esta etapa importante da minha vida, quero agradecer a todos os que contribuíram para a minha formação como pessoa e como futura profissional. Foram-me mostrados caminhos importantes a percorrer e não teria terminado o meu percurso sem a ajuda de pessoas cuja amizade, orientação e profissionalismo determinaram o sucesso desta caminhada.

Agradeço, em primeiro lugar, à Professora Doutora Maria Salomé Gomes, por me ter autorizado integrar o seu grupo de investigação, bem como me ter concedido toda a disponibilidade e oportunidades de formação e desenvolvimento, sem esquecer a preciosa ajuda na revisão desta tese.

Em segundo lugar, mas num mesmo plano de importância, o meu agradecimento é dirigido à minha orientadora, Doutora Dina Cosme, e à minha coorientadora, Doutora Ana Cordeiro Gomes, por me darem um excelente exemplo de profissionalismo, espírito crítico, perseverança, dedicação e exigência. São um exemplo a seguir tanto a nível profissional como pessoal. Agradeço toda a paciência, apoio, compreensão e ajuda que me deram de uma forma muito pessoal em todo este percurso. Agradeço por terem acreditado nas minhas capacidades e me terem ajudado a crescer de todas as formas possíveis. Agradeço todos os momentos em que me seguraram quando caía e me apoiaram no necessário crescimento profissional e pessoal. Agradeço, sobretudo, todos os conhecimentos e ensinamentos transmitidos, tanto científicos como pessoais, que nunca esquecerei na minha vida. Especialmente à Doutora Dina Cosme, agradeço por me ter ajudado a desenvolver as minhas capacidades de autonomia, de pensamento crítico, de pesquisa, de organização e comunicação científica (entre muitas outras). Agradeço ainda à Doutora Ana Cordeiro Gomes todas as oportunidades para desenvolver competências e ferramentas que me ajudarão a construir o meu caminho profissional, em particular os comentários críticos construtivos, que, como costumava dizer, me ajudarão a “brilhar”.

Quero agradecer também a todos os elementos do grupo *Host Targets of Infection*, por me fazerem sentir integrada, pela boa disposição, simpatia, espírito de ajuda e colaboração ao longo destes meses.

O meu agradecimento estende-se ainda às equipas das plataformas Proteómica e i3S, em especial ao Doutor Hugo Osório, pela sua contribuição relativa à aquisição e processamento de dados necessários à investigação. Este agradecimento inclui ainda a Dr.ª Maria Adelina Amorim, a Enfª Luciana Oliveira, a Dr.ª Rita Boaventura e a Dr.ª

Leonor Almeida, que colaboraram na recolha de amostras e tratamento de dados dos pacientes.

Um agradecimento a todos os meus amigos por todo o apoio e companheirismo ao longo de todo o meu percurso académico e pessoal. À Raquel, por ser um anjinho na minha vida, uma força nos momentos mais difíceis e por ser a minha "vizinha/parceira de laboratório" durante estes dois anos de Mestrado. À Catarina, uma das melhores surpresas que a licenciatura na FCUP me proporcionou, por ser a pessoa incrível que ilumina este mundo, e me ajudou de todas as formas possíveis. A todas as minhas amigas incríveis que fiz ao longo destes anos (especialmente à Lurdes, Leonor, Cláudia, Inês, Sofia e Gabi), que me ajudaram a trazer o melhor de mim à superfície, aceitaram as minhas falhas e esquisitices, me deram forças, me valorizaram e me encorajaram a ser o meu melhor "eu". Um agradecimento especial à Lurdes, por ter sido uma das minhas melhores amigas ao longo destes anos todos ao aturar-me, e nunca desistir de mim apesar dos meus piores momentos e do seu "busy schedule". Tenho muito orgulho em ser tua amiga. Um enorme agradecimento aos meus "cromos" (Gonçalo, Bruno, João e Diogo). Não há palavras suficientes para agradecer-vos por serem os meus companheiros, a minha plateia de todas as novidades diárias e por me fazerem sentir especial e uma de vós todos os dias. Agradeço ao, em breve, senhor engenheiro Gonçalo, por ser meu amigo há tantos anos, e por todas as gargalhadas, conversas e boleias que partilhou comigo ao longo deste percurso. Agradeço-lhe por ter-me mostrado que posso ser mais e melhor, estar sempre ao meu lado. Ao meu artista/arquiteto preferido, Bruno, agradeço-lhe por ser um verdadeiro amigo, por todos os momentos bons e pelo apoio e conforto nos momentos mais desafiantes. Ao João, agradeço todos os *nuggets* partilhados comigo durante este ano, e por todo o suporte, presença e amizade ao longo desta jornada. Ao Diogo, agradeço ser um bom amigo e me proporcionar tantos momentos de boas gargalhadas.

À minha querida amiga Professora Doutora Sónia Rodrigues, por me acolher e apoiar nos momentos mais desafiantes, e por me ajudar a redescobrir-me no meio da escuridão e mostrar-me que posso acender a vela para iluminar o meu caminho.

Aos meus tios e padrinhos, Cristina e César, por toda a preocupação e apoio que têm para comigo e por se orgulharem de mim como se fosse filha. À minha prima Isabel, por ser como uma irmã para mim, e por ser uma pessoa incrível que vai conseguir tudo de bom (e a dobrar)! Obrigada por sempre me ouvirem, proporcionarem-me bons momentos e me ajudarem a ver outras perspetivas. Aos meus avós, Artur e Anércia, que, mesmo não tendo tido a oportunidade de me ver formada, acreditaram em mim, me criaram e me apoiaram ao longo da minha vida toda. Sei que me amavam, e que

teriam tanto orgulho em mim, como o que eu tenho em ser vossa neta. À minha avó Júlia, que sempre esteve presente, sempre se preocupou e nunca duvidou de mim ou das minhas capacidades. À Leonor, Francisco, Rita, Américo, Rodrigo, Maria e Angelina, por me terem acolhido na família, me terem tratado sempre bem e me terem proporcionado tantos bons momentos ao seu lado.

Ao meu irmão Tiago, por ser o meu orgulho, o meu parceiro, o meu apoio e o meu "braço-direito" nestes últimos 19 anos. A minha vida não seria completa sem ele. Obrigada por estares lá para mim, por se preocupar e por estar sempre disponível para um abracinho quando mais precisava. Obrigada por anos de gargalhadas, piadas, jogatinas, carinho e bons momentos que partilhamos juntos. Ao acabar esta etapa, dou por mim a recordar todo o meu percurso com o meu irmão ao meu lado. Quando for a vez dele, estarei ao seu lado e mostrar-lhe-ei todo o orgulho que tenho por ele, tal como sei que ele tem por mim.

Finalmente, aos meus Pais, o meu maior *Obrigada*. Agradeço todo o amor, carinho e apoio incondicional ao longo de toda a minha existência. Obrigada por estarem presentes em todos os momentos e me terem proporcionado uma formação completa, integral, ampla, disponibilizando-me todos os meios para que eu pudesse crescer e evoluir. Vocês são o meu melhor exemplo e orgulho na minha vida. Não sei como vos agradecer toda a confiança, orgulho, força, compreensão e coragem que me foram dando ao longo desta caminhada. Obrigada por todos os pequenos mimos, os abraços e companheirismo. Obrigada por fazerem de mim a pessoa que sou, me aceitarem e me ajudarem nos meus objetivos e sonhos. Obrigada por serem o meu refúgio, a minha força e o meu lar. Amo-vos milhões.

Resumo

A fibrose quística (FQ) é uma doença multissistémica causada por mutações no gene regulador da condutância transmembranar da fibrose quística (CFTR), resultando em defeitos no canal iónico CFTR. A FQ está associada a uma maior suscetibilidade a infeções pulmonares e a perturbações na homeostasia óssea. Considerando isso, hipotetizamos que a resposta imune à colonização pulmonar, principalmente por *Pseudomonas aeruginosa* e *Staphylococcus aureus* (principais agentes colonizadores nestes pacientes), aumenta a circulação de mediadores proteicos, alterando assim a homeostasia óssea. O objetivo deste estudo foi procurar potenciais biomarcadores de saúde óssea para monitorizar a saúde óssea em pacientes com FQ e investigar o impacto molecular da infeção pulmonar bacteriana no osso destes pacientes. Para tal, o proteoma de 28 amostras de plasma de pacientes com FQ foi caracterizado. Destes 28 pacientes, 15 apresentavam massa óssea normal, enquanto os outros 13 apresentavam massa óssea baixa. Estas amostras foram posteriormente analisadas por cromatografia líquida em nanoescala acoplada a espetrometria de massa em tandem para identificar proteínas diferencialmente presentes (DPP) entre doentes com FQ com densidade mineral óssea baixa e normal. Após uma análise funcional, a proteína 88A contendo um domínio coiled-coil (CCDC88A), a proteína amiloide sérica A1 (SAA1) e a proteína morfogenética óssea 4 (BMP4) foram as DPP selecionadas como potenciais biomarcadores e foi analisada a sua correlação com a densidade mineral óssea e a função pulmonar em pacientes com FQ. Simultaneamente, macrófagos humanos foram infetados com isolados clínicos de *P. aeruginosa* ou *S. aureus* suscetível à meticilina (MSSA) de pacientes com FQ para determinar se os potenciais biomarcadores eram produzidos e/ou expressos neste tipo de células em resposta à infeção.

A CCDC88A foi menos abundante nos pacientes com densidade mineral óssea baixa em comparação com os pacientes com densidade mineral óssea normal. A SAA1 apresentou uma correlação negativa com a função pulmonar dos pacientes com FQ e foi significativamente menos abundante em pacientes com densidade mineral óssea normal tratados com ivacaftor/tezacaftor/elexacaftor (IVA/TEZ/ELE) em comparação com os não tratados. Verificou-se que o tratamento com IVA/TEZ/ELE aumenta a abundância de BMP4 em pacientes com densidade mineral óssea baixa. Para além disso, a densidade mineral óssea dos pacientes com FQ correlacionou-se positivamente com a BMP4 em pacientes sob tratamento com IVA/TEZ/ELE, enquanto a densidade mineral óssea se correlacionou negativamente com a CCDC88A em pacientes sem tratamento. A CCDC88A e a evolução da função pulmonar registaram uma correlação

negativa em pacientes com densidade mineral óssea baixa. Por outro lado, as abundâncias de SAA correlacionam-se negativamente com a função pulmonar em pacientes com densidade mineral óssea normal.

A BMP4 e as SAA1/SAA2 não foram produzidas ou expressas em macrófagos humanos infetados com isolados clínicos de *P. aeruginosa* e MSSA. No entanto, observámos uma regulação negativa da expressão de CCDC88A nestas células após a infeção por *P. aeruginosa*.

Os nossos resultados elucidaram sobre os diferentes proteomas em circulação dos pacientes de FQ osteopénicos em comparação com aqueles com massa óssea normal. Estes dados realçaram o potencial da CCDC88A, SAA1 e BMP4 como biomarcadores da saúde óssea em pacientes com FQ. A CCDC88A demonstrou potencial para a perda de massa óssea em pacientes com densidade mineral óssea baixa. Foi também observado o potencial da BMP4 como biomarcador de recuperação de massa óssea em pacientes com FQ com densidade mineral óssea baixa após o tratamento com modelador do CFTR. Além disso, observamos que a infeção por *P. aeruginosa* provoca uma regulação negativa da expressão da CCDC88A em macrófagos humanos. O nosso estudo foi o primeiro a focar-se especificamente na análise do proteoma do plasma de pacientes com FQ com diferentes massas ósseas, com o propósito de identificar biomarcadores indicativos da saúde óssea destes pacientes. A investigação de potenciais biomarcadores da saúde óssea é crucial, uma vez que são necessários métodos de diagnóstico mais simples e práticos, para diagnosticar e monitorizar a progressão da doença óssea na FQ.

Palavras-chave: Doença óssea associada à fibrose quística, Colonização pulmonar, Biomarcadores, Densidade mineral óssea

Abstract

Cystic fibrosis (CF) is a multisystemic disease caused by mutations in the cystic fibrosis transmembrane conductance regulator (CFTR) gene, resulting in defects in the CFTR ion channel. CF is associated with higher susceptibility to lung infections and hampered bone homeostasis. Considering this, we hypothesise that the immune response to lung colonisation, primarily by *Pseudomonas aeruginosa* and *Staphylococcus aureus* (main pathogens in CF patients), increases circulating mediators, thereby altering bone homeostasis. This study aimed to search for potential bone health biomarkers to monitor bone health in CF patients and investigate the molecular impact of bacterial lung infection on CF patients' bone health. To achieve this, the proteome was characterised from 28 plasma samples of CF patients. Of these 28 patients, 15 had normal bone mass, and 13 were osteopenic. These samples were then analysed by nanoscale liquid chromatography coupled to tandem mass spectrometry to identify differentially present proteins (DPP) between CF patients with low and normal bone mineral density (BMD). Following a functional analysis, the coiled-coil domain containing 88A (CCDC88A), serum amyloid A1 (SAA1) and bone morphogenetic protein 4 (BMP4) were selected as potential biomarkers, and their correlation with BMD and lung function in CF patients was analysed. Simultaneously, human macrophages were infected with CF patients' clinical isolates of *P. aeruginosa* or methicillin-susceptible *S. aureus* (MSSA) to determine whether the potential biomarkers were produced and/or expressed by this cell type in response to infection.

CCDC88A is less abundant in patients with low BMD compared to those with normal BMD. SAA1 presented negative correlation with CF patients' lung function and was significantly less abundant in normal BMD patients treated with ivacaftor/tezacaftor/elexacaftor (IVA/TEZ/ELE) compared with the untreated ones. IVA/TEZ/ELE treatment increases BMP4 abundance in patients with low BMD. Moreover, CF patients' BMD correlates positively with BMP4 in patients under IVA/TEZ/ELE treatment, whereas BMD correlated negatively with CCDC88A in patients without treatment. CCDC88A and lung function progression had a negative correlation in patients with low BMD. On the other hand, SAA abundances negatively correlate with lung function in patients with normal BMD. BMP4 and SAA1/SAA2 were not produced or expressed in macrophages infected with *P. aeruginosa* and MSSA. However, we observed a downregulation of CCDC88A expression in these cells upon *P. aeruginosa* infection.

Our results elucidated the different circulating proteomes of normal and low BMD CF patients compared to those with normal bone mass. These data highlighted the potential of CCDC88A, SAA1, and BMP4 as bone health biomarkers in CF patients. CCDC88A demonstrated potential as an indicator of bone mass loss in patients with low bone mineral density. We also observed the potential of BMP4 as a biomarker for bone mass recovery in CF patients with low BMD under CFTR modulation treatment. Additionally, we found that *P. aeruginosa* infection induces a downregulation of CCDC88A expression in human macrophages. Our study was the first to focus on the analysis of the circulating proteome in CF patients with normal and low BMD to identify biomarkers for bone health status in these patients. Therefore, the investigation of potential bone health biomarkers is crucial, as simpler and more practical diagnostic methods are needed to diagnose and monitor the progression of CF bone disease.

Keywords: Cystic fibrosis bone disease, Lung colonisation, Biomarkers, Bone mineral density

Table of Contents

List of Tables

List of Charts

List of Figures

List of Abbreviations

BMD	Bone mineral density
BMP4	Bone morphogenetic protein 4
BSL2	Biosafety level- 2
CCDC88A	Coiled-coil domain containing 88a
CF	Cystic fibrosis
CFTR	Cystic fibrosis transmembrane receptor
CFU	Colony-forming units
CRP	C reactive protein
DPP	Differentially present proteins
DXA	Dual x-ray absorptiometry
F	Femoral neck
FDR	False Discovery Rate
F508DEL	Deletion of the phenylalanine at the 508 position
GH	Growth hormone
IFN-γ	Interferon-gamma
IGF-1	Insulin-like growth factor 1
IL-10	Interleukin 10
IL-1β	Interleukin 1 beta
IL-6	Interleukin 6
IVA/TEZ/ELE	Ivacaftor/tezacaftor/elexacaftor
LC-MS/MS	Nanoscale liquid chromatography coupled to tandem mass spectrometry
LS	Lumbar spine
M-CSF	Macrophage colony-stimulating factor

MS	Mass spectrometry
MSSA	Methicillin-susceptible *Staphylococcus aureus*
NF-κB	Nuclear factor kappa B
OPG	Osteoprotegerin
PBMCs	Peripheral blood mononuclear cells
PMA	Phorbol 12-myristate 13-acetate
RANK	Receptor activating nuclear kappa-B
RANKL	Receptor activating nuclear kappa-B ligand
SAA	Serum amyloid A
TNF-α	Tumour necrosis factor alpha
%FEV1	Percentage of forced expiratory volume in the first second

1. Introduction

1.1. Cystic fibrosis: a multisystemic disease

First identified in 1938 [1], cystic fibrosis (CF) is a worldwide disease, frequently diagnosed in more developed countries due to the availability of more advanced diagnostic tools and superior medical conditions [2]. However, this disease is also recorded in other parts of the world, with an increasing incidence in Asia and Africa continents [3-6]. Over the years, the number of CF patients has increased due to the improved longevity of these individuals [7]. In 2023, Cystic Fibrosis Foundation registered 33,288 individuals with CF, with Caucasian majority (over 90%) [8]. CF is an autosomal recessive disorder caused by mutations in the cystic fibrosis transmembrane conductance receptor (CFTR) gene. This gene encodes the CFTR [2, 5, 9], described as an ATP-binding cassette transporter that functions as a chloride and bicarbonate ion channel [10, 11]. CF presents a multisystemic profile due to CFTR expression in various cells across different tissues, including the lungs, upper respiratory tract, pancreas, liver, gallbladder, intestine, sweat glands, reproductive tract and bone [2]. In CF patients, the deficiency of CFTR in the lungs and upper airways leads to the consequent formation of thick secretions and impaired mucociliary clearance. Therefore, CF patients are predisposed to chronic lung infection and recurrent acute pulmonary exacerbations [12]. Furthermore, these patients are also associated with dysregulation of the innate and adaptive immune response [5, 13, 14], with an increase in immune cells such as neutrophils and monocyte-derived macrophage accumulation in the lungs [5, 13]. This leads to advanced, end-stage bronchiectasis and progressive respiratory failure [2]. This phenomenon of hyperinflammation is related to the production of a large number of pro-inflammatory cytokines (such as Tumour Necrosis Factor α (TNF-α), interleukin (IL)-6 and IL-1β) and low levels of IL-10 [5, 14, 15].

Currently, more than 2000 mutations are known in the *CFTR* gene, but most of these mutations are extremely rare or have uncertain clinical significance. The mutations that present a clinical phenotype impact the synthesis and functionality of the CFTR channel according to the processes affected in protein production [5, 16]. CFTR mutations are conventionally organised into six different classes (Figure 1) [16, 17]: 1) Class I mutations result in early termination of transcription. These can be nonsense mutations, frameshift mutations, or mRNA splice site mutations or deletions. 2) Class II includes mutations involving CFTR protein folding. These mutations lead to defective products during protein processing in the endoplasmic reticulum (defective folding), resulting in a lower amount of CFTR protein being targeted to the cell membrane and a decrease in the correct

functionality of the protein. 3) Class III mutations are described as gating mutations. The defective regulation of the CFTR channel caused by mutations of this class leads to defective ion transport across the cell surface. These mutations allow enough CFTR protein to be present on the cell surface, even if this affects its functionality. 4) Similar to Class III mutations, Class IV mutations (called conduction mutations) result in reduced ion transport even with the normal amount of CFTR channel in the cell membrane. 5) Despite not altering the conformation of the CFTR channel, Class V mutations result in significant changes in the abundance of the protein on the cell surface since they alter the promoter regions, or splice sites, of the *CFTR* gene. 6) Finally, Class VI encompasses mutations that impair the stability of the CFTR channel in post-ER compartments and/or in the plasma membrane [2, 17]. This destabilisation contributes to an increase in the turnover of the functional protein, influencing a significant decrease in cellular ion transport.

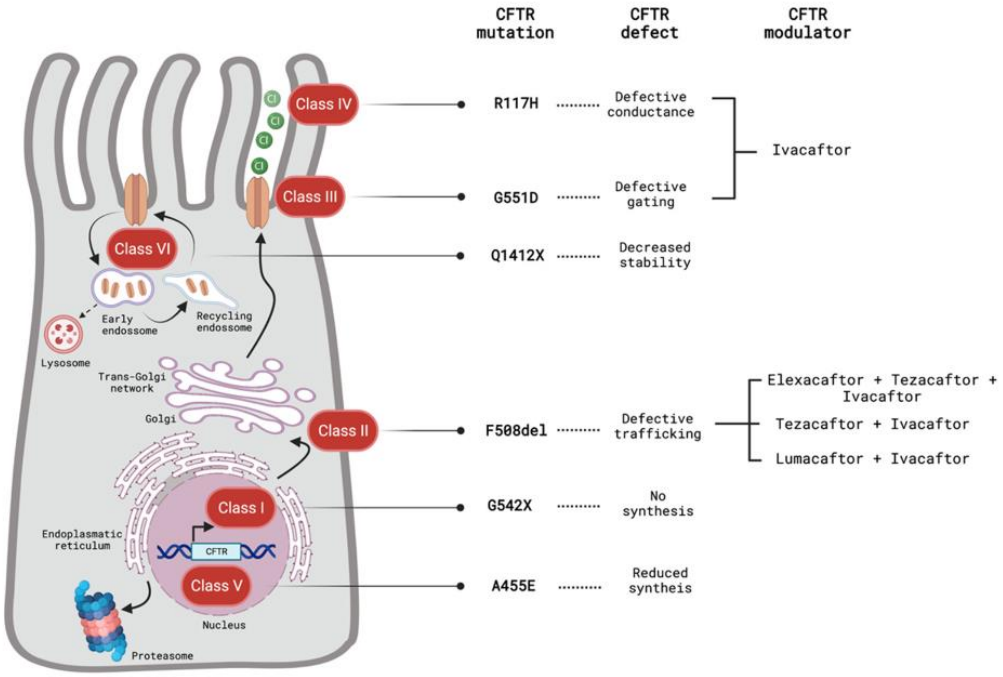

Figure 1 - Classes of CFTR mutations, the resulting channel defects, and approved pharmacological treatments for restoring CFTR function. From [5].

The phenylalanine deletion at the 508 position in the CFTR channel (F508del) is the most common mutation in CF patients. In 2022, 85.4% of individuals in the Cystic Fibrosis Foundation's patient registry annual data report were genotyped with at least one copy of this variant [6]. This Class II mutation is associated with defects in CFTR folding and impairing the correct assembly of the channel's cooperative domain [2, 17-

20]. The severity of the disease is variable in CF patients since it depends on different factors. Disease severity is mainly associated with the severity of the CFTR functional defect, but is also influenced by mutations in the promoter, intronic and exonic regions, modifier genes, the presence of two or more mutations in the same allele (which affect the function or amount of the protein), and the environmental and socioeconomic status of patients [2, 16, 17, 21, 22].

1.2 Cystic fibrosis modulator treatment

Over the years, several efforts have been made to identify directed therapies for CF. The most promising one was the modulation of CFTR channel. For that, small molecules capable to bind directly to the CFTR protein with specific site affinity during or after CFTR processing were developed. These pharmacological chaperones allowed to improve and/or to restore the CFTR function [5, 16, 17, 23]. The existence of different mutations and its combinations on CF patients led to the necessity of investigating the treatment of CF with dual or even three modulators combination [16]. Recently, the most widely used treatment is a triple combination of three modulators: ivacaftor, tezacaftor and elexacaftor [6, 16]. Ivacaftor is a highly effective CFTR potentiator that binds to the CFTR channel, allowing the mature protein to remain in an open configuration for an extended period. Elexacaftor and tezacaftor are both CFTR correctors. Tezacaftor improves CFTR protein trafficking to the epithelial cell and has the advantage of fewer drug-drug interactions. The triple action of these three molecules has improved pulmonary function, reduced the pulmonary exacerbation events and has made treatment possible for many other non-homozygous F508del patients [16]. Although this therapeutical approach has shown promising effects on the lung function and overall health of these patients, its effects on other CF related disorders are still not very clear.

1.3 Mechanism of bone homeostasis

The bone is a specialised connective tissue characterized by its strength and rigidity, which is crucial to support the body and permit its locomotion [24-26]. This tissue is very dynamic, with a high cell content and highly vascularized. The bone is capable to store cytokines and growth factors, but also calcium and phosphate, which are essential for mineral homeostasis [24, 25]. Altogether, these features are crucial to maintain an adequate bone mass, adapt to changing mechanical loads, and regenerate itself upon injury [24, 26]. The bone homeostasis is achieved by the bone remodelling, which

consists in complex processes involving a balanced forming and destruction of bone matrix by osteoblasts and osteoclasts, respectively. In the bone marrow, the mesenchymal stem cells differentiate into osteoblasts [27-29]. The osteoblasts, in turn, release essential components for bone mineralization and formation (namely collagen fibres, osteocalcin and osteonectin). Osteoblasts also produce the receptor activator of nuclear factor kappa-B ligand (RANKL) which binds to the receptor activator of nuclear factor kappa-B (RANK) on the surface of osteoclasts [29]. Additionally, osteoblasts produce a decoy receptor for RANKL named osteoprotegerin (OPG), to control osteoclast differentiation and activity. After stimulation by macrophage colony-stimulating factor (excreted by osteoblasts) and RANKL, the osteoclast progenitors formed previously from hematopoietic stem cells, differentiate into osteoclasts through fusion events and enhanced stimulation with RANKL. Osteoclasts in turn destroy the mineral matrix, through acid phosphatases-rich lysosomes and the release of cathepsin K and collagenase [24, 29, 30].

1.4 Cystic fibrosis impact on bone health

CF is associated with an imbalance in the deposition and dissolution of bone matrix that changes the bone structure in the patients, leading to bone mass loss [5, 29, 31-33]. The loss of bone mass in CF is multifactorial. Plausible causes for this phenotype include the pro-inflammatory status, long-term therapeutical therapies, chronic organ involvement, and the direct impact of CFTR dysfunction, amongst other factors (Figure 2) [5]. Moreover, the progression of osteoporosis in CF patients coincides with a worsening clinical condition [5, 34]. The worsening of the CF patients' conditions is related to the deterioration of the CF lung disease, which is associated with reduced bone mass, altered microarchitecture, imbalanced remodelling and increased microdamage in these patients [5, 35].

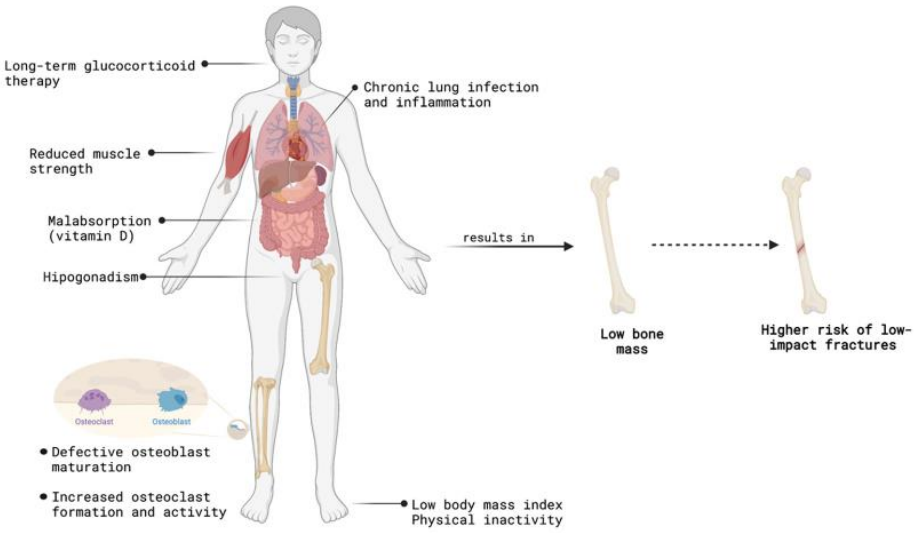

Figure 2 - Cystic fibrosis bone disease is a complex illness caused by several factors, including chronic organ involvement, the impact of CFTR malfunction on cells development alterations, immune response dysregulation and long-term treatment approaches. From [5].

The dysregulation of bone homeostasis significantly affects the lives and longevity of CF patients [5, 7, 36]. This dysregulation has been reported even in CF patients with normal nutritional status and without acute pulmonary disease [37]. In bone tissue, both osteoblasts and osteoclasts express the CFTR channel. The CFTR dysfunction compromises the osteoblasts and osteoclasts development and, consequentially, the bone remodelling [5, 38-41]. Additionally, previous studies observed that CFTR deficiency is closely involved in bone mass loss in mice [38, 42]. This bone mass loss is associated with increased bone resorption due to a higher number of osteoclasts. Additionally, bone mass formation is impaired due to decreased osteoblast formation and maturation, contributing to bone mass loss. [38, 42]. There is a correlation between the F508del mutation and low bone mass in CF patients [39, 43, 44] due to increased bone resorption and decreased new bone formation. Patients carrying the CFTR's F508del mutation exhibited a reduced expression of pro-osteoblastogenic factors (e.g., OPG) and produced increased amounts of RANKL compared with osteoblasts with a fully functional CFTR [5, 40, 45, 46]. These alterations affect various signalling pathways and protein production, correlated with decreased bone mineral density (BMD) [5, 47-51]. In CF patients with CFTR's F508del mutation, the osteoblasts present an overactive nuclear factor kappa B (NF-kB) transcriptional activity that alters the expression of Wnt/β-catenin target genes, which are essential to osteoblast maturation [47]. Additionally, TNF-α stimulation (highly produced upon infection and consequent immune response), the decreased OPG production and the CFTR function inhibition cause a decrease in

interleukin (IL) 8 secretion in osteoblasts [48]. This decrease is correlated with CF patients' femoral bone mineral density [49]. Previous studies have demonstrated that TNF-α and IL-17 stimulate the production of RANKL via osteoblasts from CF patients, which is essential for osteoclasts survival and differentiation [50]. Additionally, higher levels of macrophage colony-stimulating factor (M-CSF) receptors are expressed in monocytes from CF adults and pediatric patients [51]. The M-CSF interaction with monocytes increases their differentiation into pro-inflammatory macrophages [51] that may later differentiate in osteoclasts [29]. Although limited, some information has been observed relating to the use of CFTR modulators and their contribution to the improvement in CF bone disease. Recent studies observed the improvement in the microarchitecture of cortical bone and in BMD of CF patients when treated with ivacaftor [52, 53]. Also, the production of TNF-α and IL-17-induced RANKL was reverted upon treatment with CFTR modulator in CF patients' osteoblasts [50, 53] and the treatment with miglustat (a drug which improves F508del-CFTR function) showed to improve the bone mass in the lumbar spine and femur's microarchitecture of homozygous F508del-CFTR mice [54].

1.5. Chronical bacterial lung infection impact in cystic fibrosis patients

The CF patients defective mucociliary clearance of the airways increases the likelihood of chronic lung colonization by *S. aureus* and *P. aeruginosa* [12]. These bacteria are the most common bacterial pathogens associated with chronic lung disease in CF patients [5, 12, 55]. *P. aeruginosa* is an opportunistic, rod-shaped gram-negative bacterium that is particularly alarming due to its high mortality and morbidity rates in CF patients [56, 57]. The chronic infection with *P. aeruginosa* is associated with worsening lung function, an abnormal and persistent immune response, and significant structural changes in the lungs [12, 56-58]. Additionally, it is recommended to eradicate *P. aeruginosa* colonization in CF patients as soon as possible to preserve lung function [57]. These bacteria can penetrate into the thickened mucus plaques and produce biofilms in the hypoxic mucus zones just above the epithelial cell layer. The formation of biofilms allows the bacteria slow proliferation and creates favourable conditions for persistent infections. Furthermore, biofilm formation hinders the neutrophils' ability to penetrate the thickened mucus plaques and engulf *P. aeruginosa*, as well as impairs the diffusion of antimicrobial agents into these plaques [57, 58].

S. aureus is a gram-positive coccus bacteria that frequently colonizes the lungs of CF patients [6, 8, 59]. Like *P. aeruginosa*, this bacterium produces biofilms that are difficult to destroy once established [60]. Another worrying factor for infections with these

bacteria is the high frequency observed in patients. This is especially important for methicillin-susceptible *S. aureus* (MSSA) strain as it is the most frequently observed strain in the patients' first years of life [6, 59]. Both chronic lung infections caused by *P. aeruginosa* and *S. aureus* [12] trigger a dysregulated immune response in CF patients, characterized by the accumulation of neutrophils and macrophages in the lungs [61-63], and the excessive production of pro-inflammatory cytokines [5, 13, 61, 64]. CF patients infected with *P. aeruginosa* exhibit higher concentrations of IL-1β, TNF-α, and IL-8 in their bronchoalveolar lavage fluid [65]. Higher levels of TNF-α have been observed in CF patients with low bone density [66]. This induces osteoclast formation, influencing bone resorption and prevents osteoblast formation [5, 29, 67]. These observations suggest that the inflammatory response resulting from *P. aeruginosa* and *S. aureus* lung infections is closely associated with the production of various pro-inflammatory cytokines, leading to systemic and local bone loss [68-70]. Besides these common infectious strains, some studies have previously shown the role of other bacteria in bone degradation, associated with the inflammatory response [69, 71-74]. Mycobacterial infections have shown to influence bone loss [71]. *In vivo* experiments in mice infected with *Mycobacterium avium* have demonstrated the bone fragility in these animals compared to healthy mice [72]. Cordeiro Gomes and colleagues have reported that infection with *M. avium* is associated with increasing bone resorption and decreasing bone formation by the IFNγ- production and TNF-α secretion, which increases serum amyloid A (SAA) 3 in mice. In humans, the *SAA3* gene is described as a pseudo-gene. However, previous studies indicated that the murine *Saa3* gene and the human *SAA1* gene have evolved into functionally analogous genes, exhibiting high protein sequence homology [75]. Additionally, SAA1 and SAA2 (human homologue for SAA3) [72, 75] were shown to reduce the calcium deposits in the mice osteoblastic cultures and to increase osteoblastogenesis and osteoclast activity [72].

1.6 Proteomic analysis as a tool for biomarkers searching

Currently, various techniques for proteome analysis and quantification are widely used for various purposes, such as detecting various diagnostic markers and interpreting functional protein pathways in different diseases [76]. The first studies exploring the CF patient's proteome used "classical" techniques dependent on two-dimensional electrophoresis (2-DE) analysis to separate the proteins, followed by different possible staining methods. Then, a bioinformatic analysis and identification by Edman sequencing or mass spectrometry (MS) of the spots of interest were performed [77]. Previous studies

have already explored the use of these methods in patients with CF, to analyse the total protein expression profiles of CF versus non-CF cells [77], to search for biomarkers of CF lung disease [78], and to identify differentially expressed proteins as biomarkers of inflammation relating to pulmonary exacerbations [79]. Also, previous studies have explored techniques such as multidimensional protein identification technology, to study various aspects and mechanisms of the CFTR channel and its mechanisms [77, 80] and the protein expression profile in CF bronchial tissue comparing the CF patients with control subjects, resulting in 300 differentially regulated proteins identified, with a few of them involved in inflammation, infection and the cellular stress response [80, 81]. With technological advances, it has become possible to use more effective techniques to analyse CF proteome and protein interactions according to their biological significance and function (interactomics). These techniques permitted further studies regarding other biological perspectives such as lung proteome mapping [82], searching for treatment response blood biomarkers in CF patients with pulmonary exacerbations [83], and faecal proteome of CF patients with intestinal dysbiosis and inflammation [84]. Proteomic techniques permit proteome characterisation (both qualitatively and quantitatively) due to its unmatched ability to identify and quantify thousands of proteins [80, 85]. The versatility of proteomic analysis based on mass spectrometry to study practically any aspect of the proteome [86] constitutes an excellent approach for the study of CF to identify new disease markers with the potential to predict CF's bone mass loss. Despite these technological advances, there is still much to explore regarding the proteome of patients with cystic fibrosis.

1.7 Thesis' rational and Aims

The American Cystic Fibrosis Foundation and the European Cystic Fibrosis Society recommend the frequent monitorization of bone mineral density via a bone density scan (dual X- ray absorptiometry (DXA)) in all individuals with the disease [87-90]. Although this is a non-invasive method, the monetary cost and the patients' exposure to X-radiation [5] have some disadvantages, reducing its suitability as the primary method for frequent monitoring of these patients. This is particularly important since the decreased incidence of bone disease reported in the 2019 Cystic Fibrosis Foundation Patient Registry report [91] may be explained by the missed screening and may result in an underdiagnosis of cystic fibrosis bone disease [5]. In addition to this issue, even with no alteration in bone turnover markers levels, some studies have reported alterations in the microstructure and mineral density observed by high resolution peripheral computed

tomography and DXA, respectively [72, 92-94]. Therefore, there's a need for simpler, non-invasive and practical bone health diagnostic methods besides the common diagnosis by DXA scans [95]. This could be accomplished through soluble biomarker analysis of blood samples to verify bone condition, to predict osteopenia and low impact fractures risk. Blood samples are an excellent option due to its minimal invasive sampling nature and the blood products, such as plasma and serum, could be ideal fluids for the identification of the bone condition of these patients. Furthermore, the frequent state of lung inflammation and lungs' bacterial colonization in CF patients are key factors for the disease's severity and the various consequences it brings to patients' lives [2, 5, 12]. These observations led us to hypothesize that the bacterial infection in CF patients' lungs leads to the production and release of molecules into the circulation, potentially reaching the bone and impacting its structures and homeostasis.

In order to search for potential bone loss biomarkers, and analyse whether its production is due to bacterial lung infection, we defined the following specific aims:

1. **Search for potential soluble biomarkers of bone loss in CF patients**. For this purpose, the differentially present proteins (DPP) will be identified by proteomic analysis of CF patients' plasma with low BMD in comparison to those with a normal BMD. Then, resorting to functional enrichment, we will identify the association between the DPP and bone health. Finally, DPP will be correlated with different clinical parameters and BMD, to further investigate its association with the BMD and its potential as bone health biomarkers.
2. **Determine whether the bone-related DPP are produced by macrophages in response to bacterial infection.** For this purpose, we will enclose the establishment of *in vitro* cultures of human macrophages and their infection with CF patients' clinical isolates of *P. aeruginosa,* and *S. aureus*. Then, the production of the DPP selected as potential bone health biomarkers, will be determined at the RNA and protein levels.

2. Material and Methods

2.1. Study population

Cystic fibrosis (CF) patients with at least 18 years of age were recruited amongst the adult CF patients followed in the specialised center at Centro Hospitalar Universitário de São João (CHUSJ, Porto, Portugal), according to the study protocol approved by the Comissão Ética para a Saúde do CHUSJ (Ref. CES CHUSJ 407/21). We enrolled twenty-eight adult CF patients between February and December 2022. Patients received an information pamphlet explaining the aim of the study. They were also informed of the voluntary character of the recruitment and the minimal risks related to the venipuncture procedure. The patients signed an informed consent after agreement to take part in the study. Enrolled patients had blood samples taken and medical records reviewed. The most recent clinical information was collected by the clinician responsible for the patient enrolment and introduced in an anonymous database. The clinical data gathered included the percentage of the forced expiratory volume in the first second ($\%FEV_1$) values, and the mineral bone density obtained of the lumbar spine (LS) and the femoral (F) neck bone according to the most recent bone densitometry, amongst others. The $\%FEV_1$ variation ($\Delta\%FEV_1$) was obtained from the difference in $\%FEV_1$ values measured over an interval of time between medical consultations. The patients were grouped based on the *Z*-score value of the most recent bone densitometry, and whether these patients were treated or not with CFTR modulators, Ivacaftor/Tezacaftor/Elexacaftor (IVA/TEZ/ELE). Patients under infective exacerbation were not recruited.

2.2. Blood samples

Upon patients' informed consent, blood samples were drawn by venipuncture to EDTA coated tubes (Becton Dickson, San Jose, CA). Plasma and peripheral blood cells were separated by density gradient (Histopaque®-1077, Sigma, USA), using SepMate tubes (Stem Cell Technologies, Canada). Briefly, the blood was diluted 1:2 in PBS/2%FBS (BIOWEST, France) and transferred to a SepMate tube containing 15 ml of HistoPaque. The SepMate tubes were centrifuged at 1200 revolutions per minute (rpm) at room temperature for 10 minutes. The top layer (enriched in mononuclear cells) was poured into a new conic tube. After another centrifugation (1200 rpm for 6 minutes at 4°C), the plasma was collected and stored at -80°C until further use.

2.3. Proteomic analysis

2.3.1. Plasma sample processing for proteomic analysis

The High Select™ Depletion Spin Columns kit (Thermo Scientific, San Jose, CA) was used according to the manufacturer's instructions to exclude most abundant proteins in the plasma (e.g. albumin, IgG, IgA, IgM, IgD, IgE, kappa and lambda light chains, alpha-1-acidglycoprotein, alpha-1-antitrypsin, alpha-2-macroglobulin, apolipoprotein A1, fibrinogen, haptoglobin, and transferrin) allowing the detection the low-abundance proteins. Each sample was processed for proteomic analysis following the solid-phase-enhanced sample-preparation protocol and enzymatically digested with Trypsin/LysC as previously described [96].

2.3.2. Proteomic data acquisition

Proteomic analysis was performed by nanoscale liquid chromatography coupled to tandem mass spectrometry (LC-MS/MS) equipped with a Field Asymmetric Ion Mobility Spectrometry - FAIMS interface. This equipment is composed of a Vanquish Neo liquid chromatography system coupled to an Eclipse Tribrid Quadrupole, Orbitrap, Ion Trap mass spectrometer (Thermo Scientific, San Jose, CA). For each analysed sample, 250 nanograms of peptides were loaded onto a trapping cartridge (PepMap Neo C18, 300 µm x 5 mm i.d., 174500, Thermo Scientific, Bremen, Germany). Next, the trap column was switched in-line to a µPAC Neo 50 cm column (COL-nano050NeoB) coupled to an EASY-Spray nano flow emitter (ES993, Thermo Scientific, Bremen, Germany). A 130 minute separation was achieved by gradient phase by mixing the A component (0.1% FA) and the B component (80% ACN, 0.1% FA) at a flow of 750 µL/min, increasing the concentration of B component from 1% to 4% for 0.1 minutes, and then to 7% for 1.9 minutes. Then, the flow was reduced to 250 µL/min with increasing the concentration of component B: from 7.0 to 7.1% for 0.1 minutes, followed by an increase to 22.5% for 80 minutes. For the next 30 minutes, the component B was increased from 22.5% to 40%, and lastly, the concentration of component B was 40% to 99% for 8 minutes and maintained at that concentration for 9.9 minutes more. Next, the column was equilibrated with 1% of component B. Data acquisition was obtained using Xcalibur 4.6 and Tune 4.0.4091 software (Thermo Scientific, Germany).

Mass Spectrometry (MS) results were obtained following a Data Dependent Acquisition procedure. MS acquisition was performed with the Orbitrap detector with specific configurations: 120 000 resolution in positive mode; quadrupole isolation; scan range (m/z) 375-1500; RF Lens 30%; standard AGC target; automatic maximum injection time;

1 microscan; data type profile and without source fragmentation. FAIMS was employed with a standard resolution, at a total carrier gas flow (static 4L/min), and compensation voltage as -45, -60 and -75 (with a cycle time of one second). The Internal Mass calibration was performed as Run-Start Easy-IC. MIPS filters were used to determine the monoisotopic peak of peptides with the following parameters: charge state from 2 to 7, a dynamic exclusion of 30s, and an intensity threshold of 5.0e3. Finally, for MS/MS data acquisition, the following parameters were set: quadrupole isolation window 1.8 (m/z); higher-energy collisional dissociation (30% collision energy) as activation type; ion trap detector (IT scan rate) was used with a normal rapid mass range; scan range mode was set to auto; AGC target 100% was normalised, with a maximum injection time of 35 milliseconds, and a centroid data type.

2.3.3. Proteome data analysis

The raw data was processed using the Proteome Discoverer 3.0.1.27 software (Thermo Scientific, San Jose, CA). For protein identification, the UniProt protein sequence database for the *Homo sapiens* reviewed Proteome (2022_05 with 20,389 entries) together with human spectral library (NIST Human Orbitrap HCD 20160923) were used. A common protein contaminant list from MaxQuant was also included in our analysis. MSPepSearch and Sequest HT search engines were used to identify tryptic peptides. The ion mass tolerance used was 10 ppm for precursor ions and 0.5 Da for fragment ions. The maximum allowed missing cleavage sites was set to two. The constant modification defined was cysteine carbamidomethylation and the variable modifications defined were methionine oxidation, deamidation of glutamine and asparagine, peptide terminus glutamine to pyroglutamate, and protein N-terminus acetylation, Met-loss, and Met-loss+acetyl. Peptide confidence was set to high. The analysis also considered the enabled processing node Percolator with the following settings: maximum delta Cn 0.05; target False Discovery Rate (FDR) (strict) set to 0.01 and target FDR (relaxed) set to 0.05, with validation based on *q*-value. At the processing step, Minora feature detector node was used for protein label-free quantitation.

At the consensus step, precursor ions quantification was performed considering the unique plus razor peptides. The precursor abundance was based on intensity, and the normalization was based on total peptide amount. For hypothesis testing, a pairwise protein ratio was calculated, and a *t*-test (background based) hypothesis was performed. The differentially present proteins (DPP) were identified with the following settings:

adjusted *p*-value lesser than 0.05 and Log_2 Abundance ratios greater than 1.3, or lesser than -1.3.

2.3.4. Functional analysis

The previously mentioned DPP data were subjected to functional enrichment analysis using the functional enrichment analysis web tool WEB-based GEne SeT AnaLysis Toolkit [97] to obtain the DPP functional annotation. Then, the different patients' group DPP were inserted on the platform with their Uniprot Swiss-Prot ID and the gene ontology database was used for DPP's Over-Representative Analysis. The analysis considered the best-matched and non-contaminant proteins identified as reference.

2.4. Bacterial axenic cultures

Clinical isolates of *P. aeruginosa*, and MSSA from the CF patients were generously provided by the Microbiology laboratory of CHUSJ. From previously prepared aliquots, the bacteria were plated on LB agar (NZYTech, Portugal) and incubated overnight at 37°C. The next day, bacteria from one single isolated colony were cultured in complete RPMI medium (RPMI-GlutaMax medium supplemented with 1% HEPES 1M, 1% Non-Essential Amino Acids, 1% Sodium Pyruvate (Gibco™, Thermo Scientific, USA) and 10% FBS (BIOWEST, France)), in Erlenmeyer flasks at 37°C, 110 rpm for 18 hours. The axenic cultures of *P. aeruginosa* and MSSA were grown to exponential phase and then diluted in complete RPMI medium to reach an optical density of approximately 0.05 at 600 nm. All work with *P. aeruginosa*, and MSSA was performed inside Biosafety Level – 2 facilities (BSL2).

2.5. THP-1 cell line culture and maintenance

An aliquot of human monocyte THP-1 cells (obtained from American Type Culture Collection, Manassas, VA) was thawed under agitation in a 37°C water bath. The vial was removed from the water bath when a small frozen cell pellet remained. After decontaminating the vial with 70% ethanol, the cell suspension was transferred to a conic tube containing 14.0 mL of complete RPMI medium, supplemented with 1% Penicillin/Streptomycin (Gibco™, Thermo Scientific, USA). The tube was spun at 1200 rpm for 10 minutes. Cell pellet was resuspended in complete RPMI medium supplemented with 1% Penicillin/Streptomycin, and cells were incubated at 37°C/7% CO_2 air atmosphere at a density of 2-4 $x10^5$ viable cells/mL. THP-1 cells were

subcultured when $8x10^5$ cells/mL concentration was reached. All THP-1 cell manipulations were performed under BSL2 conditions.

2.6. THP-1 macrophages differentiation

THP-1 cells were cultured in 48 well-plate at a cell density of $1.5x10^5$ cells per well in a complete RPMI medium supplemented with 1% Penicillin/Streptomycin and 200 nM of phorbol 12-myristate 13-acetate (PMA, Sigma Merck Life Science, USA) to stimulate macrophage differentiation and incubated at 37°C/7% CO_2 air atmosphere. After three days of stimulation, the cells media were renewed with complete RPMI media supplemented with 1% Penicillin/Streptomycin. After three days of resting, the cells were ready for *in vitro* infection.

2.7. THP-1 *in vitro* infection

Macrophages were incubated with the axenic culture (previously described) of *P. aeruginosa* and MSSA for 1 hour at 37°C, 7% CO_2 atmosphere. Then, cells were washed four times with RPMI complete medium and further incubated for 30 min with 300 µg/mL of gentamycin (Duchefa Biochemie®, Netherlands) to control extracellular bacterial growth. Conditioned cell culture media of non-infected and infected cells were collected, filtrated with 0.2 µm pore size filters and stored at -80ºC. RNA extraction and intracellular bacterial load quantification were performed right after ending the infection (T0), two (T2) and four (T4) hours post-infection (described in further sections).

2.8. Quantification of bacterial load

For each time point (T0, T2, T4), three replicates of infected THP-1 derived macrophages were prepared for quantification of intracellular bacterial load. To each well, 1 mL of saline solution containing 0.05% Tween-80 (Sigma, USA) and 0.01% of saponin (Sigma, USA) was added. The wells were scraped to lyse the cells, releasing intracellular bacteria. Afterwards, the bacterial suspension was serially diluted 1:10 in a saline solution containing 0.05% Tween-80. The dilutions were plated in LB agar (NZYTech, Portugal). The plates were incubated in 37ºC for 24h. Then, colony forming units (CFUs) were counted.

2.9. ELISA

Human BMP4 and SAA1 levels were measured in the macrophage-conditioned media using human Enzyme-linked immunosorbent assays (BMP4 Human ELISA Kit, cat. no. EHBMP4 and SAA Human ELISA Kit, cat. no. EHSAA1, Invitrogen, Thermo Scientific, USA), according to the manufacturer´s instructions. The same procedure was also performed to quantify the BMP4 in cystic fibrosis patients' plasma with the same kit.

2.10. RNA isolation and quantitative real time PCR

Total RNA from non-infected and infected THP-1 macrophages from T0, T2 and T4 timepoints was isolated using RNA Mini Kit (Invitrogen), according to manufacturer's instructions. RNA was converted to cDNA using NZY First-Strand cDNA synthesis kit (NZYTech, Portugal).

The quantitative real-time PCR reactions were performed in CFX384 Touch Real-Time PCR Detection System (BioRad, USA). RT-qPCR data were analysed using BioRad CFX ManagerTM Software (BioRad, USA). Relative expression of each gene was calculated by the $2^{\Delta CT}$ method normalized to the expression of *HPRT* gene. Primers sequences are in Table 1.

Table 1 - Sequences of primers used in qRT-PCR

Gene	**Forward Primer Sequence**	**Reverse Primer Sequence**
CCDC88A	5’ – TCGTGCAAGCAGCGTGAT – 3’	5’ – TTGTTGCTCCCTAGACCTGC – 3’
BMP4	5’ – GGGATTCCCGTCCAAGCTAT – 3’	5’ – ATGGCACTACGGAATGGCTC – 3’
SAA1/2	5’- GCTACAGCACAGATCAGCAC – 3’	5’- TCCCCCGAGCATGGAAGTAT – 3’
TNF-α	5’ – CACAGTGAAGTGCTGGCAAC – 3’	5’ – AGGAAGGCCTAAGGTCCACT – 3’
HPRT	5’ –TGACCAGTCAACAGGGGACA– 3’	5’ –ATCCAACACTTCGTGGGGTC– 3’

2.11. Statistics

Data was tested for normality using the Anderson-Darling test, D'Agostino & Pearson test, Shapiro-Wilk test, and Kolmogorov-Smirnov test. When data followed a normal distribution, *t*-test or ANOVA were used to compare the experimental groups. For non-parametric data, Mann-Whitney and Kruskal-Wallis tests were used. Statistical analysis was performed using GraphPad Prism 8 (GraphPad Software, CA, USA). Spearman correlations were performed using IBM SPSS Statistics 29.0.0.0 software. A *p*-value <0.05 was considered significant.

3. Results and Discussion

3.1. The plasma proteome of CF patients differs according to BMD status

To monitor and predict bone mass loss in CF patients, we hypothesised that the identification of a protein or a set of proteins differentially present in the bloodstream of CF patients could serve as a biomarker of bone health. Thus, we used a cohort of 28 adult individuals with CF. The patients were stratified according to their BMD into 1) patients with normal BMD and 2) patients with low BMD. Then, these two groups were further stratified regarding CFTR modulator therapy: 1.1) patients with normal BMD and treated with Ivacaftor/Tezacaftor/Elexacaftor (IVA/TEZ/ELE); 1.2) patients with normal BMD and untreated with IVA/TEZ/ELE; 2.1) patients with low BMD and treated with IVA/TEZ/ELE; and 2.2) patients with low BMD untreated with IVA/TEZ/ELE (Scheme 1). The *Z*-score is a statistical measure that compares an individual's BMD with the average BMD of healthy people of the same age, gender, and ethnic background [98]. Fifteen patients with a *Z*-score value higher than -1 were grouped as normal BMD patients [88]. The remaining thirteen patients who had a *Z*-score value lower than -1 were grouped as low BMD patients [88] (Scheme 1). Among the twenty-eight patients, twelve were not treated with IVA/TEZ/ELE, while sixteen were under IVA/TEZ/ELE treatment. The median age of the CF patients was 28 years.

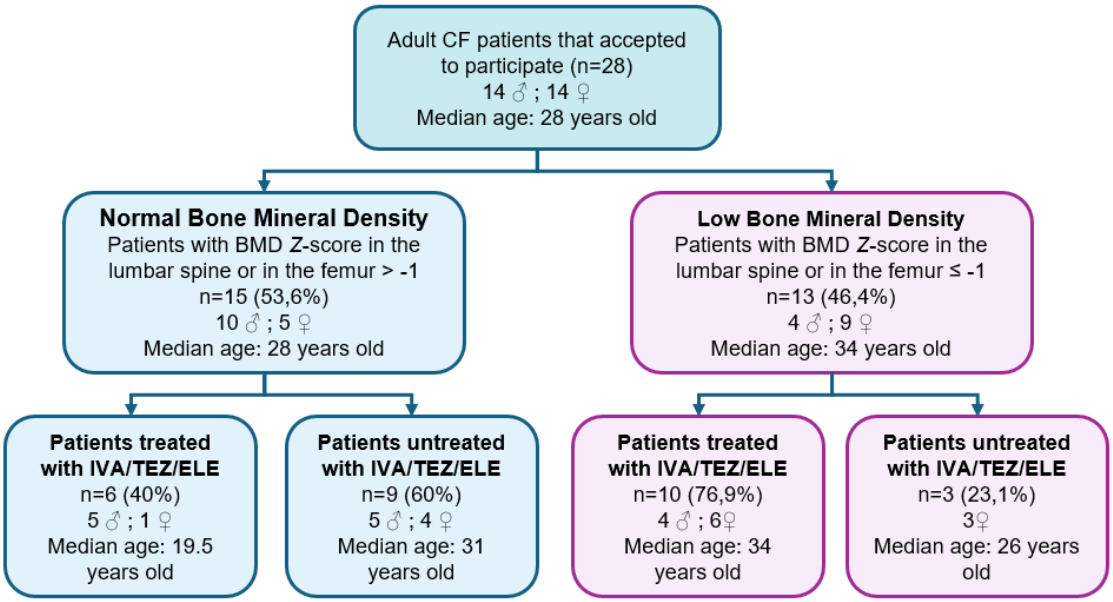

Scheme 1 - CF patients were grouped according to their bone mineral density (BMD) and IVA/TEZ/ELE treatment. The figure shows the number of patients per group, their respective percentage within the patient cohort or within the group and the median age of the individuals within each group.

After stratification for BMD and treatment, patient groups were not completely equivalent in terms of age and sex (Scheme 1). Among the normal BMD patients, there were twice as many male as female patients. In contrast, among the low BMD patients, there were twice as many female as male patients. Low BMD patients tended to be older than normal BMD patients. The proportion of patients that were under treatment was higher among those that had low BMD, as compared to those with normal BMD.

The circulating plasma proteome of the cohort was determined by nano LC-MS/MS. A total of 3112 proteins were identified amongst the 28 samples analysed. Upon removal of contaminants, the number of identified proteins was reduced to 2318. We found that 32 DPP were significantly depleted and 29 DPP were significantly enriched in low BMD patients compared to normal BMD patients (Figure 3A, Table 2). In the normal BMD group, 80 DPP were depleted and 39 DPP were enriched in IVA/TEZ/ELE treated patients compared to the untreated ones (Figure 3B, Table 3). In the low BMD group, 126 DPP were enriched and 47 DPP were depleted in IVA/TEZ/ELE treated patients (Figure 3C, Table 4). Additionally, we also compared DPP between low and normal BMD patients that were under IVA/TEZ/ELE treatment, 30 DPP were less and 73 DPP were more abundant in low BMD patients (Figure 3D, Table 5). Amongst non-treated patients, 130 DPP were more present in patients with normal BMD and 59 DPP were more present in the patients with low BMD (Figure 3E, Table 6). Overall, these results indicate that CF patients' plasma proteome differs between the patients with normal and low BMD. Additionally, we also identified that IVA/TEZ/ELE treatment alters the plasma proteome of CF patients.

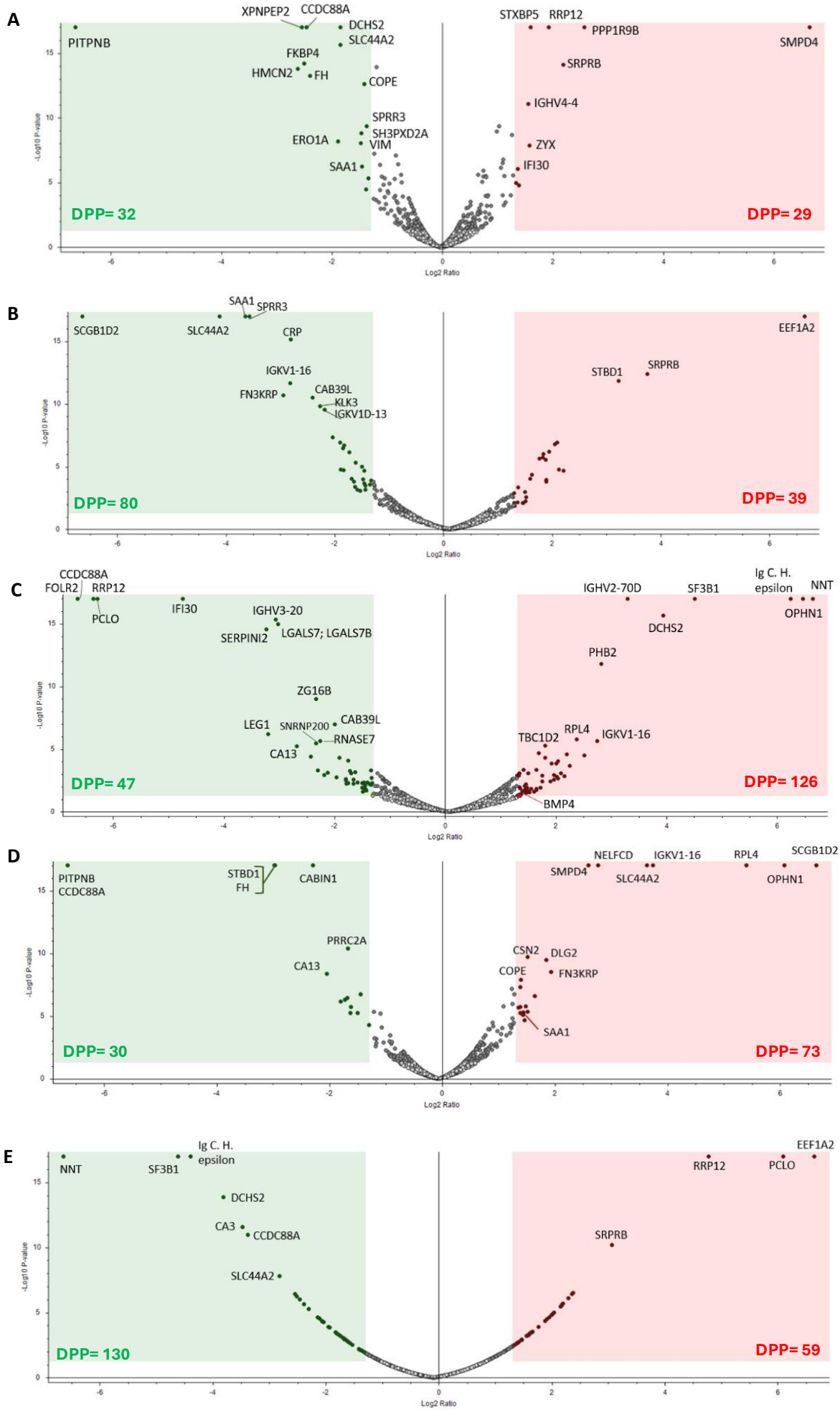
A
XPNPEP2
CCDC88A
DCHS2
SLC44A2
PITPNB
FKBP4
HMCN2
FH
COPE
SPRR3
SH3PXD2A
ERO1A
VIM
SAA1
STXBP5
RRP12
PPP1R9B
SMPD4
SRPRB
IGHV4-4
ZYX
IFI30
DPP= 32
DPP= 29
-Log10 P-value
Log2 Ratio
B
SAA1
SPRR3
SCGB1D2
SLC44A2
CRP
IGKV1-16
FN3KRP
CAB39L
KLK3
IGKV1D-13
EEF1A2
STBD1
SRPRB
DPP= 80
DPP= 39
C
CCDC88A
FOLR2
RRP12
PCLO
IFI30
IGHV3-20
SERPINI2
LGALS7; LGALS7B
ZG16B
LEG1
SNRNP200
CAB39L
RNASE7
CA13
IGHV2-70D
SF3B1
Ig C. H.
epsilon
NNT
OPHN1
DCHS2
PHB2
TBC1D2
RPL4
IGKV1-16
BMP4
DPP= 47
DPP= 126
D
PITPNB
CCDC88A
STBD1
FH
CABIN1
PRRC2A
CA13
NELFCD
IGKV1-16
RPL4
SCGB1D2
SMPD4
SLC44A2
OPHN1
CSN2
DLG2
COPE
FN3KRP
SAA1
DPP= 30
DPP= 73
E
Ig C. H.
epsilon
NNT
SF3B1
DCHS2
CA3
CCDC88A
SLC44A2
EEF1A2
RRP12
PCLO
SRPRB
DPP= 130
DPP= 59

Figure 3 **-** Volcano Plots representing the differentially present proteins (DPP) between CF patients' groups. (A) DPP between low and normal bone mineral density (BMD) CF patients. (B) DPP between IVA/TEZ/ELE-treated and untreated patients with normal BMD. (C) DPP between IVA/TEZ/ELE-treated and untreated patients with low BMD. (D) DPP between low BMD and normal BMD patients, among the patients treated with IVA/TEZ/ELE (E) DPP between low BMD and normal BMD among the untreated patients. The red areas correspond to the DPP that have a Log_2 Abundance ratio greater than 1.3 (enriched) and have a p-value lesser than 0.05. The green areas correspond to the DPP that have a Log_2 Abundance ratio lesser than -1.3 (depleted) and have a *p*-value lesser than 0.05. The number of depleted and enriched DPP in each comparison are indicated.

To the best of our knowledge, no previous proteomic comparative analysis between CF patients with different bone health status has been conducted. Moreover, although previous studies have aimed to identify biomarkers in CF patients [78, 80, 83, 99-102], this is the first study focusing on identifying biomarkers of bone health. Over the years, advancements in mass spectrometry technologies have allowed the generation of significantly more information in a faster and more efficient manner. Previous studies have undertaken various approaches to investigate the proteomic profile of different types of samples from CF patients (e.g., CF patients' nasal cells, sputum, serum, bronchoalveolar lavage fluid, bronchial epithelial cells, and plasma) compared to non-CF patients [78, 82, 83, 103-106]. Using a nano LC-MS/MS approach (the same technique we used), a previous study by Braccia and colleagues observed an upregulation of the protein COPE and a downregulation of the protein PPP1R12C using the SWATH method in bronchial epithelium of CF individuals compared to non-CF [106]. Our analyses also detected differential abundance of COPE (Tables 2-6) and PPP1R12B (a family member of PPP1R12C) [107] among CF patients, depending on BMD and treatment (Tables 2, 4, 5). The identification of these proteins in our analysis suggests that the differential expression of these proteins and/or their release to the bloodstream may be related with bone health status. Nevertheless, it is not possible to exclude that they are released into the bloodstream by cell lysis or increased necrosis, thus reflecting non-specific pathological alterations [108, 109]. C reactive protein (CRP) was also found to be differentially expressed through LC-MS/MS in CF patients' plasma throughout intravenous antibiotic therapy for pulmonary exacerbation treatment [83]. These data are consistent with what is observed in the literature, as CRP is viewed as a marker of inflammation [101], which is equally applicable to patients with CF due to their recurrent states of inflammation and infection [110]. In our study, among CF patients with normal BMD, CRP was less abundant in the plasma of those treated with IVA/TEZ/ELE, compared with those that were untreated (Table 3), suggesting that treatment decreases the inflammatory status. However, among untreated patients, CRP was less abundant in patients with low BMD than those with normal BMD, which was not expected (Table 6).

Table 2 - DPP in the plasma of CF patients with low BMD compared to CF patients with normal BMD.

↓ DPP	↑ DPP
ABCB6	ADH4
AGPS	ARAP1
AP4E1	ARMC9
ATP6V1H	CST6
BARD1	DBN1
CCDC51	GTF2E1
CCDC88A	IFI30
COPE	IGHV4-4
DCHS2	Ig heavy chain constant e
DST	KRT8
DYNLL2	MAP1A
EIF4B	MTTP
ERO1A	MYDGF
FARP1	MYH11
FH	NMD3
FKBP4	OPHN1
GLUD1	PCBP1
HMBS	PPP1R12B
HMCN2	PPP1R9B
Keratin-8-like protein 1	RASA1
PITPNB	RRP12
PRDX3	SEMG2
PRORP	SMPD4
SAA1	SPRR4
SDK1	SRPRB
SH3PXD2A	STXBP5
SLC44A2	TMEM41A
SPRR3	ZSWIM9
Uncharacterized protein FLJ45252	ZYX
USP15	
VIM	
XPNPEP2	

DPP depleted (↓ DPP) and DPP enriched (↑ DPP) in low BMD CF patients compared with normal BMD patients. The proteins in bold were studied as potential bone health biomarkers.

.

Table 3 - DPP in the plasma of CF patients with normal BMD under IVA/TEZ/ELE treatment compared to untreated normal BMD patients.

↓ DPP		↑ DPP
ABCC2	MRPS34	ANKRD22
ACTBL2	MTTP	APOA5
ALPL	MYH11	ATP13A1
ARMT1	NAA15	CABIN1
AXL	NAMPT	CUL5
BPTF	NCOA6	CYGB
BRK1	NELFCD	DLG5
CAB39L	NT5C2	DTNB
COPE	NUCB2	EEF1A2
CRNN	PCMTD1	EIF3B
CRP	PDS5A	ETFA
CSTA	PKMYT1	FREM2
DCHS2	POF1B	GYG1
DIPK2A	PRDX3	H2BC20P
DLG2	PRKCSH	HNRNPA1
DSC3	RBM39	KALRN
DST	RNASE7	MCM6
DYNLL2	RPL4	MTHFR
EMP2	RRP12	NOL9
EPHX2	S100A14	NUMA1
ERO1A	**SAA1**	NUP188
FBP1	SBSN	PALD1
FKBP4	SCGB1D2	PCBP1
FLNB	SERPINA12	PHB2
FN3KRP	SERPINB2	PPM1A
GALK2	SERPINI2	PPP1R9B
GLUD1	SH3PXD2A	PRORP
HDGF	SLC25A1	RAB5C
HMBS	SLC44A2	RAD23B
IFI30	SPRR3	SDK1
IGHV3-20	TMEM41A	SMPD4
IGKV1-12	TMX2	SPCS1
IGKV1-16	TNRC6B	SRPRB
IGKV1D-13	TRIM28	STBD1
IGKV2-29	Uncharacterized protein FLJ45252	STXBP5
Ig heavy chain constant e	USP15	THNSL1
Keratin-8-like protein 1	VSIG4	WRAP73
KLK3	XPNPEP2	ZC3H18
KRT3	XPOT	ZMPSTE24
LGALS7; LGALS7B	ZNF446	

DPP depleted (↓ DPP) and DPP enriched (↑ DPP) in IVA/TEZ/ELE-treated compared to untreated normal BMD patients. The proteins in bold were studied as potential bone health biomarkers.

Table 4 - DPP in the plasma of CF patients with low BMD under IVA/TEZ/ELE treatment compared to untreated low BMD patients.

↓ DPP		↑ DPP				
ABCC2	PIWIL1	ABTB3	DDX6	IGLV3-16	OGFOD1	SSR3
ACAA1	PPM1A	ACTN3	DIPK2A	IGSF1	OPHN1	STBD1
AGR3	PPP1R9B	ADGRF5	DST	Ig heavy chain constant e	OXCT1	STXBP5
AHNAK	PRKCSH	ADGRG6	DTNB	IMPA2	PALD1	TANGO2
ARAP1	PRKDC	AGPS	EBP	INTS4	PDK1	TBC1D2
ARMC9	RAD23B	AGTRAP	EIF3F	ITGA1	PHB2	THNSL1
ARMT1	RNASE7	APOA5	EPHA1	KALRN	PIAS1	TMX2
CA13	RRP12	APOBEC3G	ETFA	KCNAB2	PKMYT1	UBR4
CAB39L	SCGB1D2	ATP13A1	EXT2	KIF13B	PPP1R12B	UGT2A3
CCDC88A	SERPINB12	B4GALT1	F2RL3	KRT8	PRKACA	Uncharacterized protein FLJ45252
CST6	SERPINB13	C19orf47	FAM83B	L2HGDH	PRKAR2B	UPF2
EIF3B	SERPINH1	C1orf131	FARP1	LGMN	PTPN4	VIM
EMP2	SERPINI2	CABIN1	FH	LHFPL2	PTPRC	VPS29
FOLR2	SETMAR	CAMSAP2	FKBP4	MANBA	PWP2	ZZZ3
GTF2E1	SNRNP200	CBLN1	GOLGA2	ME1	PYCR2	
GYG1	TMEM41A	CDH1	GPT2	MEMO1	QSER1	
HDHD2	UGT1A1	CEMIP2	H2BC20P	MRM2	RCN1	
IFI30	ZG16B	CENPB	HDGF	MRPS34	RECK	
IGHV3-20	ZNF446	CLEC4M	HMBS	MTTP	REP15	
IGLV10-54		CMTR2	HMCN2	MYH6	RPA1	
ITIH5		COL14A1	HNRNPA1	NAMPT	RPL4	
LEG1		COPE	ICOSLG	NCOA6	SEMG2	
LGALS7; LGALS7B		CPT2	IGHV1-58	NDRG2	SERPINB4	
MAP1A		CTSS	IGHV2-70D	NELFCD	SF3B1	
MCM6		CTSZ	IGHV4-39	NEO1	SH3PXD2A	
NDFIP1		CUL5	IGKV1-16	NNT	SLC38A7	
PCLO		DCAF1	IGKV2-29	NUDC	SPCS1	
PDS5A		DCHS2	IGLV1-44	NUMA1	SPRR4	

DPP depleted (↓ DPP) and DPP enriched (↑ DPP) in treated with IVA/TEZ/ELE low BMD CF patients compared to untreated low BMD patients. The proteins in bold were studied as potential bone health biomarkers.

Table 5 - DPP in the plasma of CF patients with low BMD IVA/TEZ/ELE-treated compared to normal BMD IVA/TEZ/ELE-treated patients.

↓ DPP	↑ DPP		
ACAA1	ACTN3	IGKV2-29	SERPINI2
AHNAK	ALPL	Ig heavy chain constant e	SH3PXD2A
AP2B1	ARMT1	KRT3	SLC44A2
ATP6V1H	AXL	KRT8	SMPD4
CA13	BPTF	LGALS7; LGALS7B	SPRR3
CABIN1	C19orf47	MAP1A	SPRR4
CCDC51	COPE	MRPS34	TMX2
CCDC88A	CPT2	MTTP	TNRC6B
EIF4B	CRNN	MYDGF	Uncharacterized protein FLJ45252
FARP1	CSN2	MYH11	VSIG4
FH	CST6	NAA15	XPNPEP2
FOLR2	DBN1	NAMPT	XPOT
GYG1	DCHS2	NCOA6	ZNRD2
HAPLN3	DIPK2A	NELFCD	
HDHD2	DLG2	NT5C2	
MCM6	DSC3	NUCB2	
NKRF	DST	OPHN1	
PITPNB	EIF3D	PCMTD1	
PPP1R9B	EMP2	PKMYT1	
PRKACB	EPHX2	POF1B	
PRORP	ERO1A	PPP1R12B	
PRRC2A	FKBP4	PRKCSH	
PTPRC	FLNB	RBM39	
RAD23B	FN3KRP	RPL4	
SDK1	GALK2	S100A14	
SERPINB13	HDGF	**SAA1**	
SLC38A7	HMBS	SCGB1D2	
STBD1	IFI30	SEMG2	
USP15	IGKV1-12	SERPINA12	
ZNF446	IGKV1-16	SERPINB2	

DPP were less (↓ DPP) and more abundant (↑ DPP) in treated with IVA/TEZ/ELE low BMD CF patients compared to treated normal BMD patients. The proteins in bold were studied as potential bone health biomarkers.

Table 6 - DPP in the plasma of CF patients with low BMD and untreated with IVA/TEZ/ELE compared to patients with normal BMD patients and untreated with IVA/TEZ/ELE

↓ DPP					↑ DPP		
ABTB3	DCAF1	ICOSLG	MTTP	PYCR2	ACAA1	LEG1	SRPRB
ACTN3	DCHS2	IGHV1-58	MYH6	QSER1	ADH1B	LGALS7; LGALS7B	TTC27
ADGRF5	DDX6	IGHV2-70D	NAMPT	RCN1	ADH4	MAP1A	UGT1A1
ADGRG6	DIPK2A	IGHV4-39	NDRG2	RECK	ARAP1	MCM6	ZG16B
AGPS	DST	IGHV5-10-1	NELFCD	REP15	ARHGAP18	MTHFR	ZMPSTE24
AGTRAP	DYNLL2	IGKV1-16	NEO1	RPA1	ARMC9	MYDGF	ZNF446
APOBEC3G	EBP	IGKV1D-13	NKRF	**SAA1**	ARMT1	PCBP1	ZYX
ATP6V1H	EIF3F	IGKV2-29	NNT	SERPINB4	CALM3	PCLO	
AXL	EIF4B	IGLV1-44	NT5C2	SF3B1	CBR1	PDAP1	
B4GALT1	EPHA1	IGLV3-16	NUDC	SH3PXD2A	CRYZL1	PIP	
BRK1	ERO1A	IL36A	OGFOD1	SLC25A1	CST6	PIWIL1	
C1orf131	ETFA	Ig heavy constant Δ	OSMR	SLC38A7	DBN1	POF1B	
CA3	EXT2	Ig heavy chain constant e	OXCT1	SLC44A2	DDX10	PPM1A	
CABIN1	FAM83B	IMPA2	PALD1	SPCS1	DOK3	PPP1R9B	
CAMSAP2	FARP1	ITGA1	PDK1	SSR3	EEF1A2	PRKDC	
CBLN1	FGL1	ITGAL	PHB2	STBD1	EIF3B	QARS1	
CCDC51	FH	Keratin-8-like protein 1	PIAS1	TACC1	EIF3D	RAB5C	
CCDC88A	FKBP4	KIF13B	PITPNB	TANGO2	EPHX2	RNPEP	
CDH1	FN3KRP	KLK3	PKMYT1	TMX2	GTF2E1	RPN2	
CEMIP2	GLUD1	LGMN	PLXNB2	TRMT11	GYG1	RRP12	
CENPB	GOLGA2	LHFPL2	PRDX3	Uncharacterized protein FLJ45252	IFI30	SAG	
COL14A1	GPT2	MANBA	PRKACB	USP15	IGHV3-20	SCGB1D2	
COPE	HDGF	ME1	PRKAR2B	VIM	IGHV4-4	SETMAR	
CPA4	HMBS	MEMO1	PTPN4	VPS29	IGKV3D-7	SMPD4	
CRP	HMCN2	MRM2	PTPRC	XPNPEP2	KLC4	SNRNP200	
CTSZ	ICAM1	MRPS34	PWP2	ZZZ3	KRT3	SPP2	

DPP were less present (↓ DPP) and DPP were more present (↑ DPP) in untreated with IVA/TEZ/ELE low BMD CF patients compared to untreated normal BMD patients. The proteins in bold were studied as potential bone health biomarkers.

3.2. Functional enrichment analysis of the differently present proteins in CF patients did not reveal biological functions directly related to bone loss.

After the proteome analyses of the different patient groups, we investigated whether the identified differently present proteins had functions related to bone health. For this purpose, a functional enrichment analysis was performed to investigate the biological functions of DPP between the different CF patients' groups using the WEB-based GEne SeT AnaLysis Toolkit. Interestingly, no enriched biological functions were directly related to bone metabolism or homeostasis. The enriched biological functions were globally related to intracellular functions, namely remodelling/organisation of the cytoskeleton, protein modification and transport (Figures 4 and 5). Compared to normal BMD patients, the depleted proteins (Figure 4A) and the enriched proteins in low BMD patients (Figure 4B) have similar intracellular functions, including remodelling/organisation of the cytoskeleton content, protein modification and transport, nervous system regulating processes, and DNA related processes. However, the detection of these proteins in the bloodstream is puzzling and might be explained by the cell lysis or increased necrosis [108, 109]. Nevertheless, the plasma of low BMD patients´ proteome shows a depletion of proteins involved in metabolic functions (Figure 4A) and an enrichment for proteins involved in the regulation of GTPase activity (Figure 4B). Several metabolic processes are diminished in patients with low BMD, particularly the tricarboxylic acid and tetrapyrrole metabolic processes (Figure 4A). Although no direct relation between these processes and bone mass loss in CF patients has been reported, the depletion of the identified DPP (GLUD1, FH, HMBS, ABCB6) (Figure 4A) may indicate a reduction of these metabolic processes in those CF patients. These potentially affected processes may lead to an imbalanced redox homeostasis, an altered Krebs tricarboxylic acid cycle in the mitochondria [111-113], a reduced heme biosynthetic pathway [114], and ATP transport in cells [115]. Although there is no apparent direct link between these factors and bone mass loss, it has been previously reported that CF patients have a deficit of antioxidant molecules and an increase in oxidative stress [116]. In turn, these lead to a sustained imbalance between oxidant and antioxidant species, sustaining chronic inflammation [116]. This is in line with the literature, as chronic inflammation in CF patients is significantly related to bone mass loss through the production of pro-inflammatory cytokines that alter bone homeostasis [5].

The differential presence of the GTPase-activating proteins OPHN1, RASA1, and ARAP1 (Figure 4B) demonstrates an enrichment in pathways involved in the control Rho

GTPases activity [117-120]. Small GTPases are associated with the stimulation of osteoclast differentiation and function, promoting bone mass loss in these patients [121, 122]. Therefore, the enrichment of GTPase activity regulation in low BMD CF patients may represent a mechanism to prevent further bone mass loss in these patients. Of note, IVA/TEZ/ELE treatment depletes proteins related to cell cycle arrest, protein alkylation and the somatic diversification of immune receptors (Figure 4C) in low BMD patients. On the other hand, IVA/TEZ/ELE treatment increases proteins related to hormone-mediated signalling pathways and leukocyte activation during inflammatory response (Figure 4D), which may be related to the improvement on the overall health status of CF patients under IVA/TEZ/ELE treatment [16, 110].

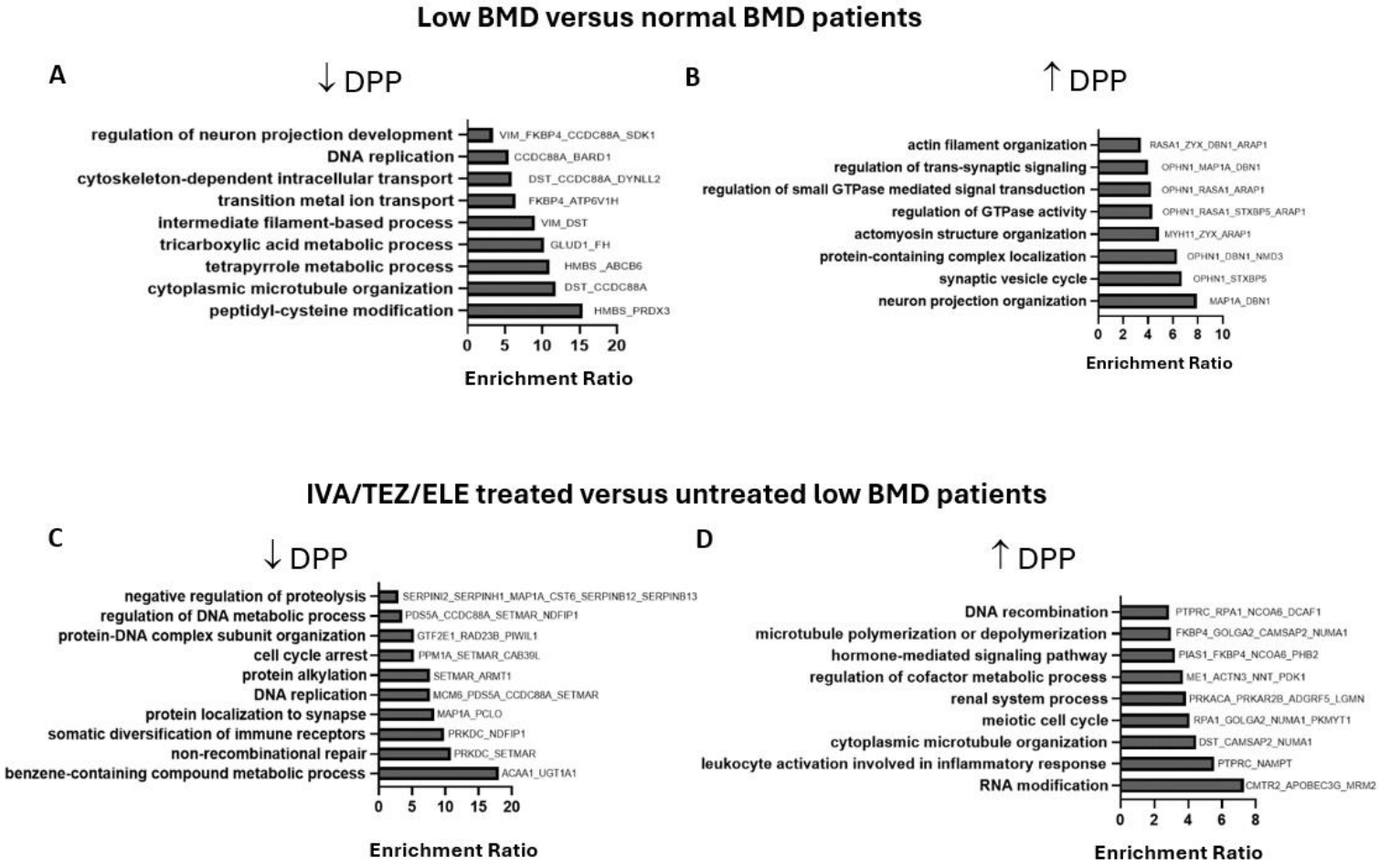

Figure 4 - Functional analysis of DPP in low BMD CF patients. The most significant biological processes of the depleted (A) and enriched (B) DPP in low BMD patients compared with normal BMD patients; and the depleted (C) and enriched (D) DPP in low BMD patients treated with IVA/TEZ/ELE compared with those without treatment. Each column represents a significant biological process with their respective enrichment ratio and the proteins that contribute to these processes.

Then, we aimed to determine whether the functions of DPP were different between low and normal BMD patients after restoring CFTR function (i.e, patients under IVA/TEZ/ELE treatment). Again, DPP were not directly related to bone metabolism and/or homeostasis (Figure 5A and 5B). The enriched DPP in low BMD IVA/TEZ/ELE-treated patients contribute to protein-containing complex localization and negative regulation of proteolysis (Figure 5B). However, in untreated patients, low BMD was associated with a depletion in proteins related with cytoplasmic microtubule organization, leukocyte activation in inflammatory response and RNA modification (Figure 5C). Low BMD and reduced CFTR function were also associated with an increase in proteins related to hormone metabolism (Figure 5D). The DPP associated with hormone metabolism process (ZMPSTE24, ADH4, ACAA1, and UGT1A1) are not reported to have a direct relationship with bone metabolism. However, previous studies have shown that *Zmpste24*-deficient mice exhibit increased activation of autophagic processes linked to alterations in lipid and glucose metabolic pathways and changes in blood parameters such as leptin, insulin, glucose, and adiponectin [123]. *Zmpste24*-deficient mice also showed alterations in genes regulating the somatotroph axis, alongside elevated circulating levels of growth hormone (GH) and reduced plasma levels of insulin-like growth factor 1 (IGF-1) [124]. GH and IGF-1 were reported to enhance bone turnover and formation by stimulating the proliferation, differentiation, and activity of osteoblasts and osteoclasts [125]. Thus, there may be a relationship between the function of ZMPSTE24 and the IGF/GH balance [124], which could impact bone turnover [125]. Other matched DPP were ADH4, ACAA1, and UGT1A1 that are involved in alcohol metabolism [126, 127], the beta-oxidation system of peroxisomes [128, 129], and the glucuronidation of numerous endobiotics, xenobiotics, and drugs for excretion [130, 131]. Thus, these proteins may be potentially linked to other clinical aspects of the multisystemic nature of the disease besides the CF bone disease [2]. Another curious biological function performed by these differentially present proteins is protein alkylation (Figure 5D). This function may be associated with an attempt by these patients to rescue CFTR activity, even without treatment. Previous studies found that some C-alkyl azepanes show significant rescue of F508del-CFTR activity despite being less efficient than miglustat [132], an α-glucosidase inhibitor has previously shown to rescue the defective F508delCFTR function significantly [133].

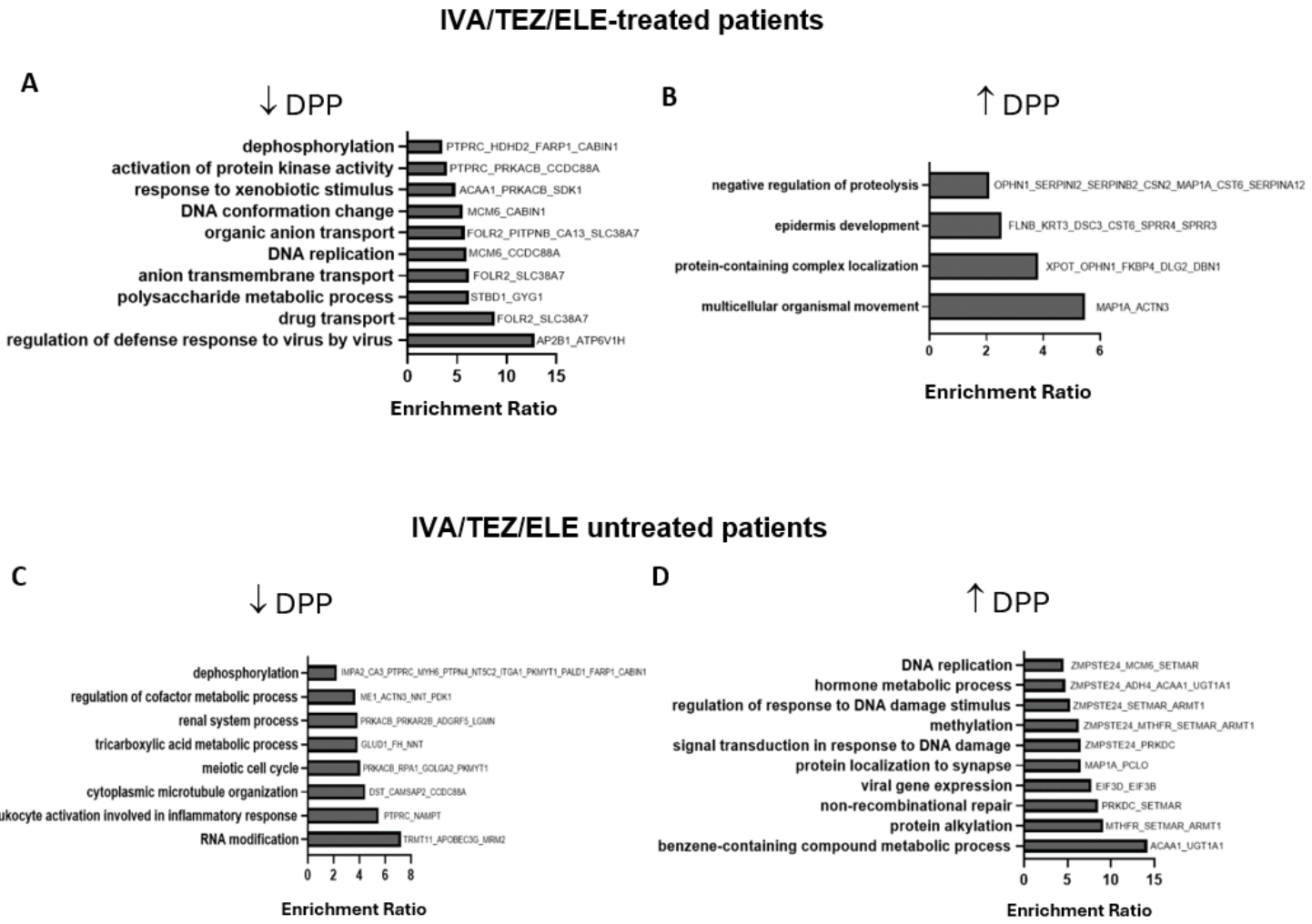

Figure 5 - Functional analysis of DPP in low versus normal BMD patients, stratified according to treatment. The most significant biological processes of the depleted (A) and enriched (B) DPP in low BMD patients with IVA/TEZ/ELE treatment compared with normal BMD treated with IVA/TEZ/ELE; the depleted (C) and enriched (D) DPP in low BMD patients without IVA/TEZ/ELE treatment compared with normal BMD without IVA/TEZ/ELE treatment. Each column represents a significant biological process, with their respective enrichment ratio and the proteins that contribute to these processes.

Throughout the analysis of DPPs and their biological functions among the patient groups, it was observed that different proteins were significantly enriched or depleted in various CF groups' proteomic comparisons. Thus, three proteins raised our interest: the coiled-coil domain containing 88A (CCDC88A), serum amyloid A1 (SAA1), bone morphogenetic protein 4 (BMP4), which will be explored in the next section.

3.3. CCDC88A, BMP4 and SAA1 were identified as potential biomarkers of bone health

We selected potential bone health biomarkers based on the following criteria: their association with low bone mass patients, their relevance to bone-related processes, their biological functions, and their frequent appearance in the proteomic and functional enrichment analysis. CCDC88A stood out for being involved in several biological processes among different CF patients' groups (Figures 4 and 5, Table 2, Table 4, Table 5 and Table 6). CCDC88A is essential for the integrity of the actin cytoskeleton and cell migration, and it is identified as a critical regulator of both physiological and pathological processes [134, 135]. Despite its physiological roles, such as regulating the migration of various cells by modifying the actin-binding protein Akt [136], its significant frequency in our analyses underscores its potential importance as a biomarker. Firstly, CCDC88A is depleted in low BMD CF patients compared to normal BMD patients (Figure 3A, Table 2). This protein participates in different biological pathways, such as regulation of neuron projection development, DNA replication, cytoskeleton-dependent intracellular transport, and cytoplasmic microtubule organisation (Figure 4A). These biological functions presented enrichment ratios of 3.38, 5.49, 5.92, and 11.83, respectively. Moreover, CCDC88A was also depleted in low BMD patients treated with IVA/TEZ/ELE compared to untreated patients (Figure 3C, Table 4), which was associated with regulation of the DNA metabolic process and DNA replication with enrichment ratios of 3.54 and 7.72, respectively (Figure 4C). The depletion of CCDC88A was also observed in the low BMD patients treated with IVA/TEZ/ELE (Figure 5A) compared with normal BMD treated patients. Overall, these results suggest that CCDC88A depletion correlates with bone health status of CF patients independently of IVA/TEZ/ELE treatment. In the patients with low BMD and under IVA/TEZ/ELE treatment, CCDC88A associated with activation of protein kinase activity and DNA replication, having enrichment values of 3.97 and 5.95, respectively (Figure 5A). Finally, CCDC88A was grouped in the organization of cytoplasmic microtubule (enrichment ratio 4.44) in low BMD untreated patients compared with normal untreated patients (Figure 5C). CCDC88A is involved in multiple cellular vesicular trafficking, especially in endosomes and autophagosomes [137]. Previous studies reported the contribution of CCDC88A on Akt-mTOR signalling pathway [138, 139], which has been shown to contribute to bone regeneration and angiogenesis [140]. Taking this relationship into account, this suggests that reduced levels of CCDC88A lead to a decrease of this pathway, and therefore contribute to osteopenia [141]. Furthermore, the relative abundance of CCDC88A was reduced in CF patients with low BMD (Figure 6A). Further stratification by treatment revealed that the

relative abundance of CCDC88A in normal BMD patients treated with IVA/TEZ/ELE were reduced compared to untreated normal BMD patients (Figure 6B). Of note, CCDC88A was not detected in the low BMD and IVA/TEZ/ELE treatment group. The data suggest that CCDC88A has potential as a biomarker of bone loss, since it is reduced in low BMD patients, and its abundance levels do not seem to be restored in patients treated with IVA/TEZ/ELE (Figure 6B).

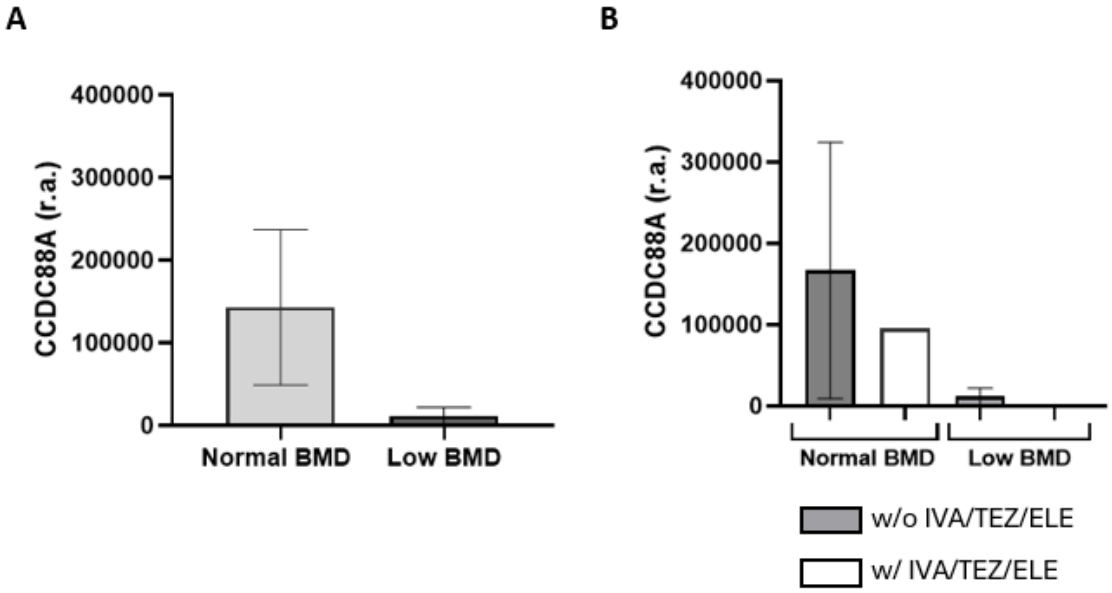

Figure 6 - Low bone mineral density (BMD) cystic fibrosis (CF) patients have less CCDC88A than normal BMD patients. (A) Columns represent the CCDC88A relative abundance (r.a) average in normal BMD CF patients (light grey column) and in low BMD CF patients (dark grey column). (B) Columns represent the CCDC88A r.a. average in normal and low BMD patients with or without CFTR modulator treatment. Darker grey columns represent the untreated patients in each normal and low BMD group. White columns represent the treated patients in each normal and low BMD group. Bars indicate the standard error of the mean. Abbreviations: w/o IVA/TEZ/ELE = patients without IVA/TEZ/ELE treatment; w/ IVA/TEZ/ELE = patients with IVA/TEZ/ELE treatment.

Secondly, we identified the SAA1 protein as a DPP in CF patients (Figure 3A, 3B, 3D, Table 2, Table 3, Table 5). SAA1 were depleted in low BMD patients compared with the normal BMD patients (Figure 3A, Table 2). However, when patients were stratified by IVA/TEZ/ELE treatment, this protein was enriched in normal BMD patients untreated with IVA/TEZ/ELE compared to treated patients (Figure 3B, Table 3). Additionally, among patients receiving IVA/TEZ/ELE treatment, low BMD patients exhibited enriched SAA1 compared to normal BMD patients (Figure 3D, Table 4). SAA proteins are acute phase proteins that are expressed mostly by macrophages in the liver [142], but also in other tissues and cell types, like human monocytes and macrophages, chondrocytes, adipocytes, and osteoblasts in response to inflammatory stimuli [72]. Human SAA1 and

SAA2 are homologous to mouse SAA3, which was previously shown to interfere with bone homeostasis, impairing osteoblast differentiation and increasing osteoclast activity [72, 75, 143]. Cordeiro Gomes and colleagues demonstrated that the production of SAA3 in response to *M. avium* infection, dependent on the cytokines IFN-γ and TNF-α, increases osteoclast activity and decreases osteoblastogenesis [72]. Considering the relationship between SAA, inflammatory cytokines and infection, SAA proteins may serve as biomarkers of bone loss in CF patients, who often experience chronic lung infections and subsequent bone mass loss [12, 61, 72]. The relative abundances of SAA1 in the normal BMD group were higher than low BMD patients (Figure 7A). Then, considering IVA/TEZ/ELE treatment in low and normal BMD patients, the SAA1 relative abundance in patients with normal BMD and under treatment with IVA/TEZ/ELE was significantly lower (Figure 7B). In addition, treated and untreated low BMD patients showed very low SAA1 relative abundance values (Figure 7B). These results indicated that IVA/TEZ/ELE treatment reduces the SAA1 levels in normal BMD. However, this effect is not observed in the low BMD group (Figure 7B). Recent studies have reported that inflammatory stimuli increase the response to CFTR modulators *in vitro* and *in vivo* [144, 145]. Also, combinations of CFTR modulators have potent anti-inflammatory properties [146], which greatly improve the lung function of CF patients [16, 146]. SAA1 not only is an inducible acute phase protein in response to injury, infection, and inflammation, but also stimulates the production of proinflammatory cytokines [147]. It has also been reported to be elevated in serum during inflammation and interacts with immune cells through inflammatory chemokines [148, 149]. The reduction of SAA1 was expected with the IVA/TEZ/ELE treatment due to its anti-inflammatory effect, which decreases SAA1 levels by reducing inflammation. Additionally, these results show that monitoring the inflammatory state may be a relevant tool to predict the loss of bone mass in these patients.

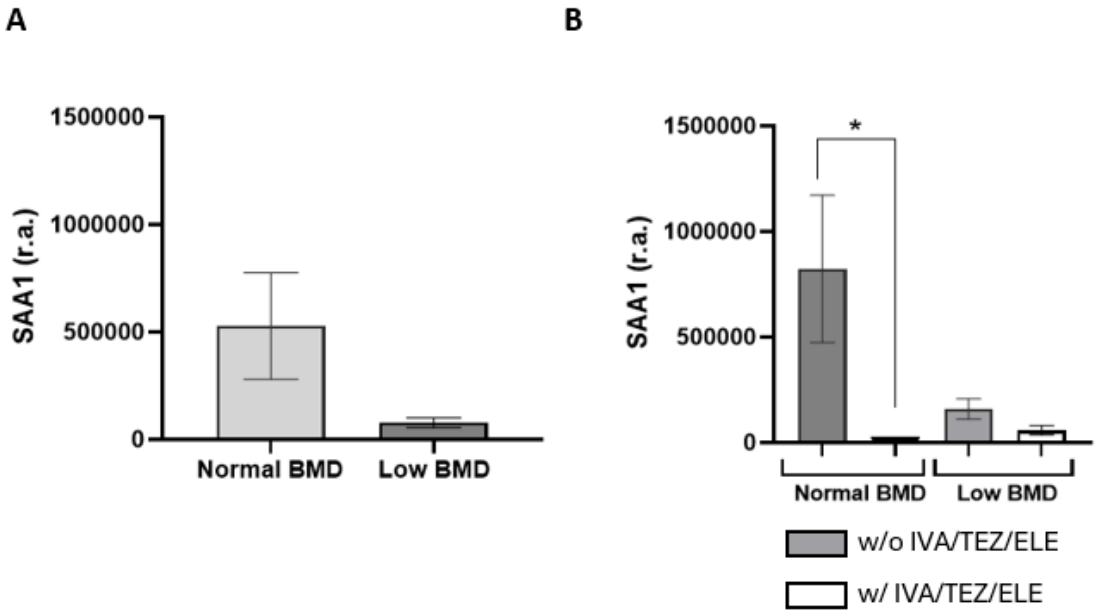

Figure 7 - Normal bone mineral density (BMD) CF patients present higher SAA1 relative abundance than low BMD patients. (A) Columns represent the SAA1 relative abundance (r.a) average in normal BMD patients (light grey column) and low BMD patients (dark grey column). (B) Columns represent the SAA1 r.a. average in normal and low BMD patients with or without CFTR modulator treatment. Darker grey columns represent the untreated patients in each normal and low BMD group. White columns represent the treated patients in each normal and low BMD group. Bars indicate the standard error of the mean. *p<0.05 by two-way ANOVA, followed by Kruskal-Wallis multiple comparison test. Abbreviations: w/o IVA/TEZ/ELE = patients without IVA/TEZ/ELE treatment; w/ IVA/TEZ/ELE = patients with IVA/TEZ/ELE treatment.

BMP4 raised our interest due to its role in the bone development and enrichment in low BMD treated with IVA/YEZ/ELE (Figure 3C). BMP4 is a multifunctional cytokine [150, 151] highly related to bone due to its role as an osteogenic factor [152, 153] and its requirement for osteoblastogenesis [154, 155]. The relative abundance of BMP4 was slightly and not significantly increased in the low BMD group (Figure 8A). When stratified by IVA/TEZ/ELE treatment, the normal BMD patients who received treatment exhibited a slight but not statistically significant increase in the relative abundance of BMP4 compared to untreated normal BMD patients (Figure 8B). Interestingly, amongst the CF individuals with low BMD, those under IVA/TEZ/ELE treatment had higher abundance of BMP4 (Figure 8B). Previous studies have reported the positive effects of ivacaftor treatment on bone mineral density by improving the microarchitecture of cortical bone [5, 52, 53]. Despite not statistically significant, normal BMD patients under IVA/TEZ/ELE treatment had slightly increased levels of BMP4 (Figure 8B) compared with the untreated patients. Therefore, the increase in BMP4 abundances in IVA/TEZ/ELE treated patients support the potential use of BMP4 as a response biomarker, after restoring CFTR modulation in the CF patients with low BMD. Then, we directly quantified the BMP4

circulating levels using an ELISA assay and no significant differences were observed between CF patient groups (Figures 8C and 8D). This may be attributed to the insufficient sensitivity of the ELISA assay kit used, as the absorbance readings of the samples were below the detectable range defined by the absorbance of the first standard provided in the kit (data not shown).

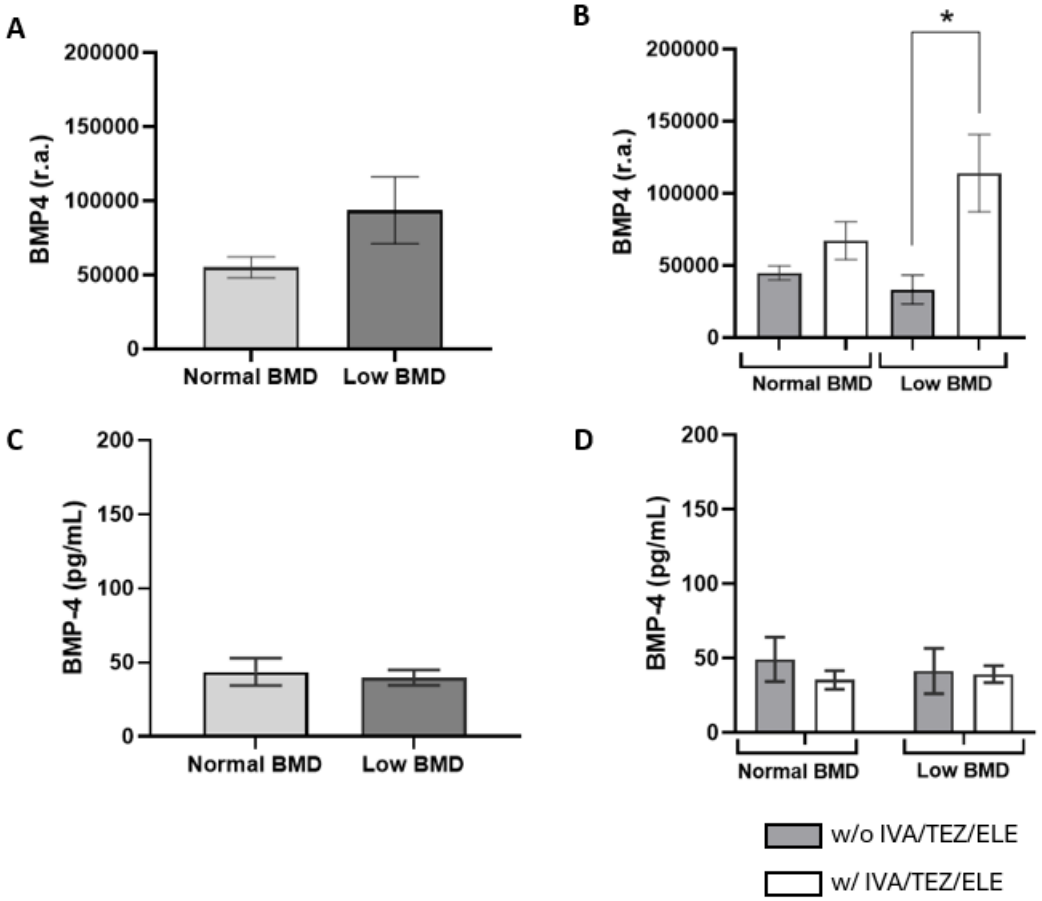

Figure 8 **-** Normal and low bone mineral density (BMD) CF patients present differences in BMP4 relative abundance. (A) Columns represent the BMP4 relative abundance (r.a.) average in normal BMD patients (light grey column) and low BMD patients (dark grey column). (B) Columns represent the BMP4 r.a average in normal and low BMD patients with or without CFTR modulator treatment. Darker grey columns represent the untreated patients in each normal and low BMD group. White columns represent the treated patients in each normal and low BMD group. (C) Columns represent the average BMP4 circulating levels in normal BMD patients (light grey column) and low BMD patients (dark grey column) measured by ELISA assay. (D) Columns represent the average BMP4 circulating levels in normal and low BMD patients with or without CFTR modulator treatment. Darker grey columns represent the untreated patients in each normal and low BMD group. White columns represent the treated patients in each normal and low BMD group. Bars indicate the standard error of the mean. *p<0.05 by two-way ANOVA, followed by Kruskal-Wallis multiple comparison test. Abbreviations: w/o IVA/TEZ/ELE = patients without IVA/TEZ/ELE treatment; w/ IVA/TEZ/ELE = patients with IVA/TEZ/ELE treatment.

3.4. CCDC88A, SAA1 and BMP4 correlate with bone mineral density and lung function in CF patients.

We investigated whether the relative abundances of CCDC88A, SAA1 and BMP4 correlated with BMD in lumbar spine and femoral neck of CF patients. For this purpose, Spearman´s rho correlation analysis was performed for the different patients' groups. BMP4 relative abundances positively correlated with BMD values in the lumbar spine of patients with normal BMD (Figure 9). This finding was expected as BMP4 is highly associated with bone development in several studies throughout the literature [152-157]. On the other hand, CCDC88A negatively albeit weakly correlated with BMD both in the lumbar spine and femur neck of both group of patients (Figure 9). This relationship indicates that patients with poorer bone mass have higher abundance of CCDC88A. We initially expected a positive correlation between the CCDC88A abundance and CF patients' BMD, since CCDC88A could contribute to the Akt-mTOR signalling pathway [138, 139], which could increase bone regeneration [141]. However, this inverse correlation between the abundance of CCDC88A and BMD leads us to think that this relationship does not contribute to the improvement of bone health, and therefore, patients with low BMD exhibit less CCDC88A. This can be explained by the fact that previous studies have demonstrated that targeting the PI3K/Akt/mTOR signalling pathway increases CFTR stability and expression by restoring autophagy through the inhibition of mTOR [158]. This might indicate that the reduction of CCDC88A is part of a mechanism to stabilize CFTR through mTOR inhibition. Therefore, the relationship between CCDC88A and BMD remains unclear. Interestingly, other DPP (CAB39L, PDK1 and PPM1A (Tables 3, 4 and 6)) were also related indirectly with mTOR signalling pathway [159-162]. Based on this, it seems that the relationship between CCDC88A and BMD of CF patients is not based on a direct association with the CCDC88A protein, but rather on its contribution to the mTOR signalling pathway. This reinforces the relevance of this pathway to the understanding and complexity of CF disease [158, 163-165].

Interestingly, SAA1 relative abundances positively correlated with BMD in the femur neck of normal BMD patients and with BMD in the lumbar spine of low BMD patients (Figure 9). These results were opposite from what we expected. Previous studies demonstrated that human SAA proteins impair bone matrix deposition and increase osteoclastogenesis *in vitro* [72], resulting in bone mass loss.

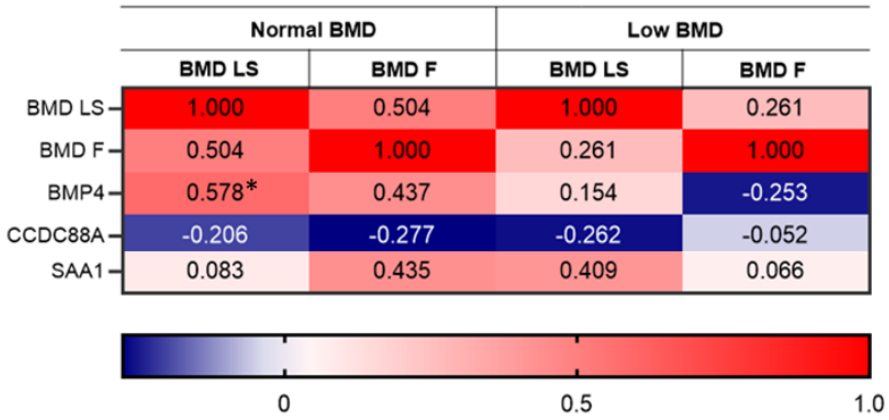

Figure 9 - Non-parametric Spearman´s rho correlations between bone mineral density (BMD) in lumbar spine (LS) and femur neck (F) and CCDC88A, SAA1 and BMP4 abundances in normal and low BMD CF patients' groups. Spearman's rho was converted in color from blue to red and significance within positive or negative correlations were shown as *, $p<0.05$.

In addition to the loss of bone mass, one of the major clinical problems of CF is the decline in lung function due to recurrent or chronic bacterial and fungal infections [2, 12, 166]. The bone mass loss and the decline of the lung function are closely related as low BMD patients present a more severe disease [167]. The forced expiratory volume in the first second (FEV_1) is an index of airway obstruction, used as the primary spirometric result of interest in both clinical care and research in CF [168]. To understand whether the relative abundance of CCDC88A, SAA1 and BMP4 correlated with the lung function progression, we correlated the relative abundance of these proteins with the variation of the percentage of FEV1 ($\Delta\%FEV_1$,). The $\Delta\%FEV_1$ in low BMD patients had a positive but weak correlation with BMP4 abundances. We observed a significant moderate negative correlation between $\Delta\%FEV_1$ and CCDC88A abundances in low BMD patients. SAA1 abundances had a moderate but significant negative correlation with lung function progression in the patients with normal BMD but weakly correlated in the low BMD patients (Figure 10).

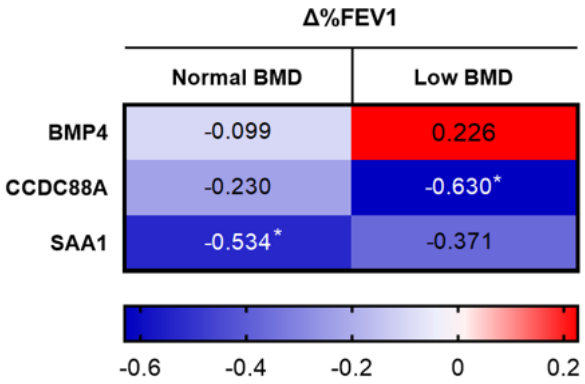

Figure 10 - Non-parametric Spearman´s rho correlations between lung function and CCDC88A, SAA1 and BMP4 abundances in normal and low BMD CF patients' groups. The lung function is observed through the variation of the percentage of forced expiratory volume in 1 second (Δ%FEV1). Spearman's rho was converted in colour from blue to red and significance within positive or negative correlations were shown as *, $p<0.05$.

It is known that the treatment improves lung function in patients with CF [16]. Therefore, we conducted a second correlation analysis to investigate the relationship between the improvement in lung function and the abundances of BMP4 and CCDC88A in patients stratified by IVA/TEZ/ELE treatment (Figure 11). We observed a significant strong positive correlation between BMP4 abundances and lung function progression in low BMD untreated CF patients (Figure 11). The positive correlations of BMP4 with lung function indicated a positive relationship between this protein and the improvement of pulmonary function in CF patients with low BMD (Figures 10 and 11). This is further reinforced by the fact that BMP4-mediated modelling of the SMAD signalling pathway has already been reported to enhance lung cell differentiation [169], which in turn may relate to the recovery of lung function through those cells.

Interestingly, the negative correlation between CCDC88A and low BMD patients' lung function was maintained after stratification by treatment (Figure 11). A perfect negative correlation was observed between CCDC88A abundances and lung function in low BMD untreated CF patients. This result may be due to a previous observation that reported that an inhibition of the mTOR pathway improved CFTR channel stability in patients with the CFTR' F508del mutation [158]. In addition, previous studies have shown that inhibiting the mTOR signalling pathway reduces pulmonary complications during injurious ventilation [170]. Furthermore, the mTOR signalling pathway has also been associated with pulmonary alterations in chronic obstructive pulmonary disease and lung cell senescence [171]. Therefore, this may suggest an indirect relationship between CCDC88A and BMD through the mTOR signalling pathway. Overall, we found that low

CCDC88A levels are associated with low BMD patients, and higher levels are associated with worse pulmonary function (Figures 5, 6, 10 and 11). To our knowledge, this is the first study that associates CCDC88A with BMD and lung function in patients with CF. Further studies are required to understand the mechanisms behind these associations.

A moderate negative correlation between SAA1 abundances in low BMD untreated patients and lung function was found. The negative correlation between SAA1 abundance levels and lung function (Figures 10 and 11) is consistent with previous findings, indicating that elevated SAA1 levels associated with inflammation lead to a decline in CF patients' lung function. [5, 148, 149]. Overall, the results of the proteomic analysis and the Spearman correlations (Figures 3, 7, 10, and 11) indicated that SAA1 could serve as a lung function biomarker in CF patients with normal BMD. This could be particularly beneficial by reducing the need for patients to undergo spirometry, saving both time and resources since these patients are already subjected to blood tests analysis [6]. Instead, lung function could be assessed through the analysis of circulating SAA1 levels through blood analysis.

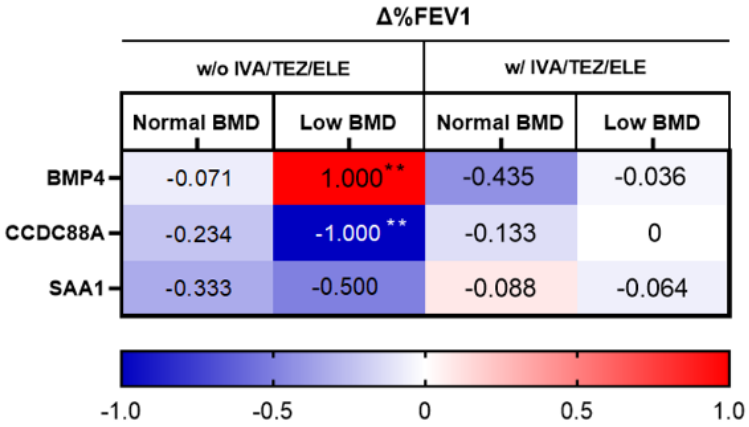

Figure 11 - Non-parametric Spearman´s rho correlations between lung function and CCDC88A, SAA1 and BMP4 abundances in normal and low BMD CF patients' groups stratified by IVA/TEZ/ELE treatment. The lung function is observed through the variation of the percentage of forced expiratory volume in 1 second (Δ%FEV1). Spearman's rho was converted in colour from blue to red and significance within positive or negative correlations were shown as *, $p<0.05$ and **, $p<0.01$. Abbreviations: w/o IVA/TEZ/ELE = patients without IVA/TEZ/ELE; w/ IVA/TEZ/ELE = patients with IVA/TEZ/ELE treatment.

3.5. *CCDC88A* is downregulated in THP-1 macrophages infected with *P. aeruginosa in vitro*

CF patients are predisposed to chronic lung infections caused by *P. aeruginosa* and *S. aureus* [12], which leads to the accumulation of macrophages in their lungs [61]. We hypothesized that the chronic lung colonization by these bacterial pathogens in CF patients leads to the production of soluble mediators by alveolar macrophages and impact bone homeostasis [5]. To test this hypothesis, THP-1 monocytes were differentiated *in vitro* into macrophages [172] and infected with CF clinical isolates of *P. aeruginosa* and MSSA [173]. The initial bacterial load (T0) and the intracellular bacterial load two hours (T2) and four hours (T4) post infection were quantified. In *P. aeruginosa*, 5.9% of the initial bacterial load was internalized by the THP-1 derived macrophages (Figure 12A). The macrophages remained infected with the bacteria throughout the procedure, demonstrating that we established an effective infection model. The intracellular bacterial load was very similar between T0 and T2 time points. The bacterial load increased slightly from T2 to T4 time points (Figure 12A) although there was no statistical significance. In the *S. aureus in vitro* infection, 6.3% of the bacteria were internalized after infection, with no increase observed from the time immediately after infection (T0) to the subsequent hours (T2 and T4) (Figure 12B). In both infection models, it was not possible to test beyond four hours of infection time as the cells lost their viability due to the bacterial growth.

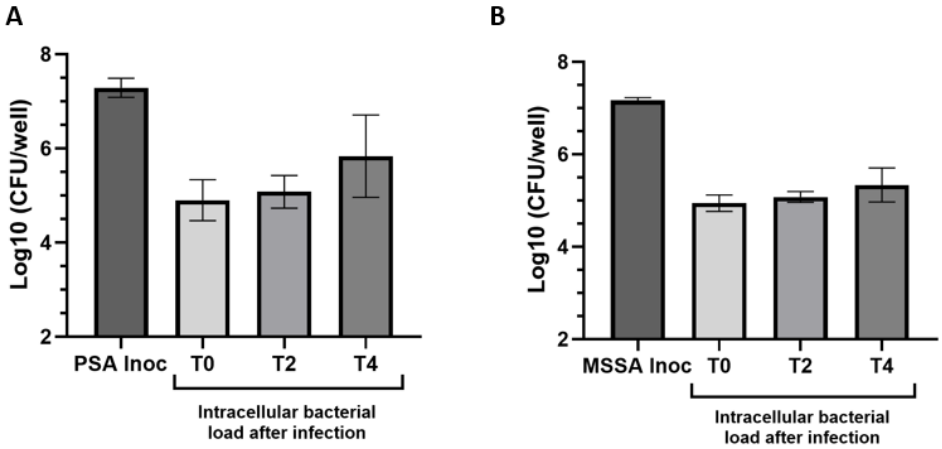

Figure 12- Quantification of *P. aeruginosa* and MSSA load in THP-1 derived macrophages by Colony-Forming Units (CFUs). *P. aeruginosa* (A) and MSSA (B) initial bacterial load (PSA Inoc and MSSA Inoc, respectively), and intracellular bacterial load right after THP-1 infection (T0), and two (T2) and four (T4) hours after infection. Columns represent the experimental conditions values average (n=4 for macrophage infection with *P. aeruginosa,* n=3 for macrophage infection with methicillin-susceptible *S. aureus*). Bars indicate the standard deviation.

Then, we collected culture's supernatant and RNA to determine whether CCDC88A, BMP4 and SAA1 were produced in response to infection. We were unable to quantify the levels of BMP4 and SAA1 by ELISA in the supernatants of infected and non-infected cultures due to values below the detection limit. Then, we analysed the expression of *SAA1/SAA2, BMP4, CCDC88A* and *TNFα* by RT-qPCR. The expression of *TNFα* was measured as a positive control since this gene is known to be expressed upon bacterial infection [174, 175] and downregulated over time after infection [176]. The expected downregulation of *TNFα* in THP-1 derived macrophages was observed (Figures 13A and 14A). This is consistent with previous data of our group, where TNFα levels were increased in the circulating peripheral blood mononuclear cells (PBMCs) and plasma of CF patients with low BMD (Cosme et al, in preparation).

P. aeruginosa and MSSA infection in THP-1 derived macrophages did not lead to significant expression of *BMP4* (data not shown). These results were expected, since BMP4 is expressed mainly in mesenchymal stem cells and chondrocytic cells [177, 178]. *P. aeruginosa* infection did not induce *SAA1/SAA2* expression in THP-1 derived macrophages (Figure 13B).

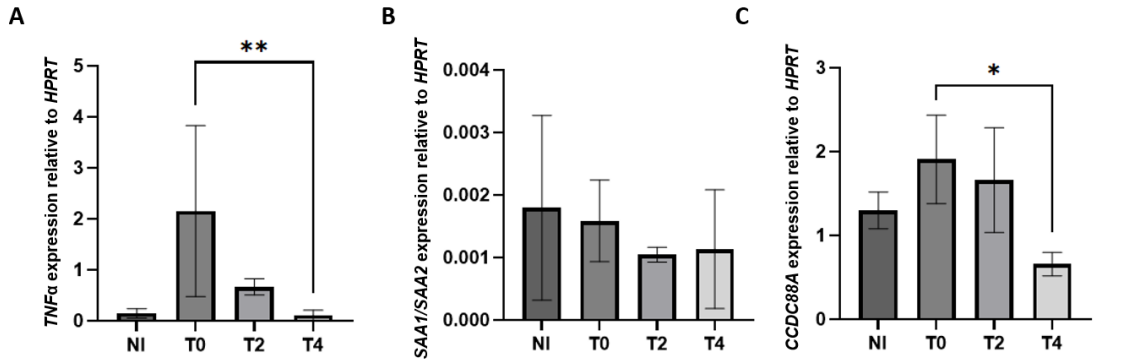

Figure 13 - *SAA1/SAA2*, *CCDC88A* and *TNFα* expression in non-infected THP-1 derived macrophages and after *P. aeruginosa in vitro* infection. (A) *TNFα* expression relative to *HPRT* in THP-1 derived macrophages. (B) *SAA1/SAA2* expression relative to *HPRT* in THP-1 derived macrophages (C) *CCDC88A* expression relative to *HPRT* in THP-1 derived macrophages. Columns represent the experimental conditions values average (n=4 for macrophage infection with *P. aeruginosa).* RNA extraction was performed in non-infected THP-1 derived macrophages (NI) and in infected macrophages right after infection (T0), two (T2) and four (T4) hours after infection with *P. aeruginosa*. Bars indicate the standard deviation. **p*<0.05 by one-way ANOVA, ***p*<0.01 by one-way ANOVA.

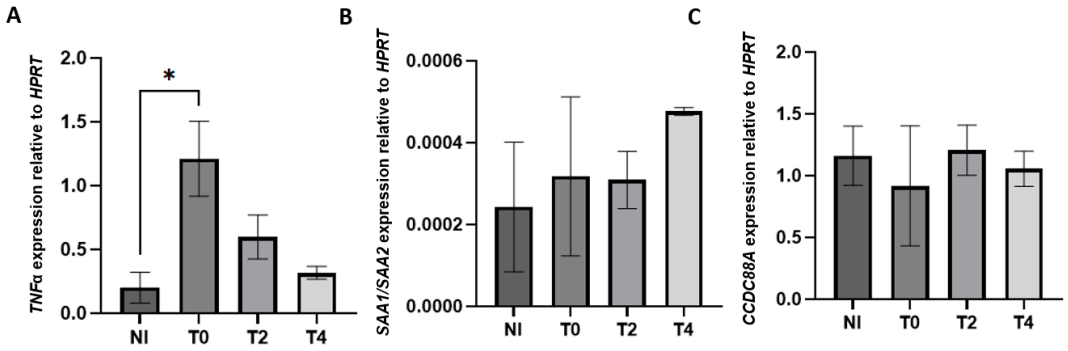

Figure 14 - *SAA1/SAA2*, *CCDC88A* and *TNFα* expression in non-infected THP-1 derived macrophages and after MSSA *in vitro* infection. (A) *TNFα* expression relative to *HPRT* in THP-1 derived macrophages. (B) *SAA1/SAA2* expression relative to *HPRT* in THP-1 derived macrophages (C) *CCDC88A* expression relative to *HPRT* in THP-1 derived macrophages. Columns represent the experimental group's average (n=3 for macrophage infection with methicillin-susceptible *S. aureus)*. RNA extraction was performed in non-infected THP-1 derived macrophages (NI) and in infected macrophages right after infection (T0), two (T2) and four (T4) hours after infection with MSSA. Bars indicate the standard deviation. *p<0.05 by one-way ANOVA, followed by Kruskal-Wallis multiple comparison test.

S. aureus infection slightly but not significantly increased SAA1/SAA2 expression at four hours after infection (Figure 14B). This is an unexpected result, since previous studies found an increased expression of the *SAA* gene in human monocytes and macrophages after stimulation by LPS treatment [148], and in bone marrow-derived macrophages, five days after *M. avium* infection in mice [72]. However, our results showed that *SAA1/SAA2* are not upregulated in response to *P. aeruginosa* and only slightly upregulated in MSSA infection in human macrophages over the four hours after infection. Nevertheless, considering these results, it will be worth investigating in the future whether the expression of SAA proteins are increased in response to mycobacterial infections in human macrophages, since this type of bacteria also affects the CF patients [6, 8].

CCDC88A expression was significantly downregulated in the following hours after *P. aeruginosa* infection (from T0 to T4) (Figure 13C). This differential gene expression was not observed when the cells were infected with MSSA (Figure 14C). This protein showed a downregulation pattern similar to that observed in *TNF*α (Figure 13A and 13C). To our knowledge, no differences in *CCDC88A* expression with *P. aeruginosa* infections have been reported to date. This is the first time that expression of this protein was studied in human macrophages post infection. It is known that CFTR loss in macrophages impacts their ability to resolve *P. aeruginosa* infection [13, 179]. In addition to the higher production of pro-inflammatory cytokines/chemokines in response to bacterial infection [13, 15, 180], macrophages with CFTR loss exhibit altered biological processes and pathways [179, 181]. Despite the complexity of the mTOR signalling pathway in

macrophages, it is established that this pathway can exert context-dependent effects on the regulation of macrophage activation [182]. Another significant aspect is the effect of mTOR signalling pathway inhibition to increase the CFTR stability and expression in CF bronchial epithelial cells expressing ΔF508 CFTR mutation [158]. Thus, a hypothesis can be formulated regarding the decrease of *CCDC88A* in macrophages upon *P. aeruginosa* infection. Considering the increased cytokine production and impaired infection resolution by CFTR-deficient macrophages [15], restoring CFTR stability and expression through mTOR signalling pathway inhibition, via *CCDC88A* downregulation, might mitigate the negative impacts observed in CFTR-deficient macrophages in response to infection. This could lead to better infection resolution and reduce excessive cytokine production. Consequently, this might decrease bone mass loss in CF patients by reducing the hyperinflammatory state frequently observed in these patients [5]. However, it is uncertain the effects of mTOR signalling pathway inhibition given the complex role of this pathway in macrophages [182]. Nevertheless, it would be worthwhile to further investigate the impact of *CCDC88A* downregulation in CFTR-deficient macrophages, its implications for the inflammatory state of these patients, and its effect on bone health. Moreover, prior analyses showed a downregulation of CCDC88A in PBMCs of CF patients compared to non-CF patients (Cosme et al, in preparation). However, the same experiment would need to be conducted in CFTR-deficient cells. This could be achieved by using a cell line with these characteristics, as we previously tried to differentiate PBMCs from CF patients into macrophages, but we have not been successful. It would be particularly interesting to perform CCDC88A analysis by stratifying CF patients *by P. aeruginosa* colonisation.

4. Final Remarks

This study provided extensive and novel data regarding the proteome of CF patients with low BMD. Subsequent functional analysis of this data revealed that DPP perform various biological functions, essentially related to intracellular processes. Based on their biological functions and differing abundances among CF patients, CCDC88A, SAA1, and BMP4 were identified as potential biomarkers of bone health. CCDC88A abundance was reduced in CF patients with low BMD, independently of CFTR modulation (Scheme 2A). From our analyses, a decrease in CCDC88A may alert for bone mass loss. SAA1 is less abundant in normal BMD patients treated with IVA/TEZ/ELE compared with the untreated ones (Scheme 2A). Additionally, this protein was correlated with patients' $\Delta\%FEV_1$, suggesting its utility as a pulmonary function biomarker in these patients. We then observed higher levels of BMP4 in low BMD patients treated with IVA/TEZ/ELE (Scheme 2A). Our analysis suggests that BMP4 has potential as a biomarker to monitor bone formation in CF patients with low BMD following IVA/TEZ/ELE treatment. Overall, our results reveal these proteins' potential as biomarkers for BMD loss and formation, as well as for the worsening of lung function in CF patients.

Additionally, we found that *in vitro* infection of human macrophages by *P. aeruginosa* or MSSA did not significantly induce the production or expression of SAA1/SAA2 and BMP4 (Scheme 2B). However, *P. aeruginosa* infection downregulates *CCDC88A* expression (Scheme 2B). This finding suggests that the effects of *CCDC88A* downregulation could be further investigated, particularly in relation to CF disease.

A

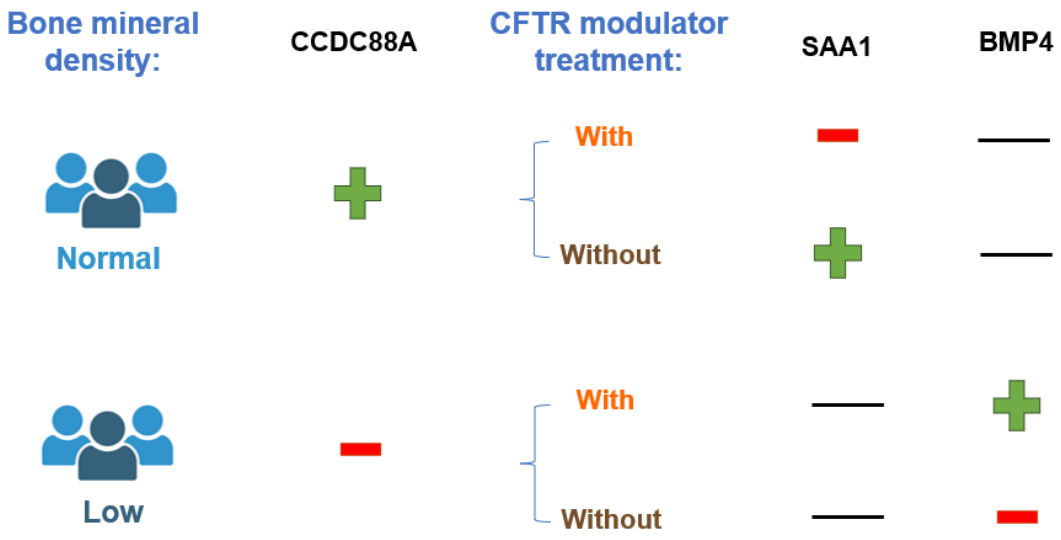

B

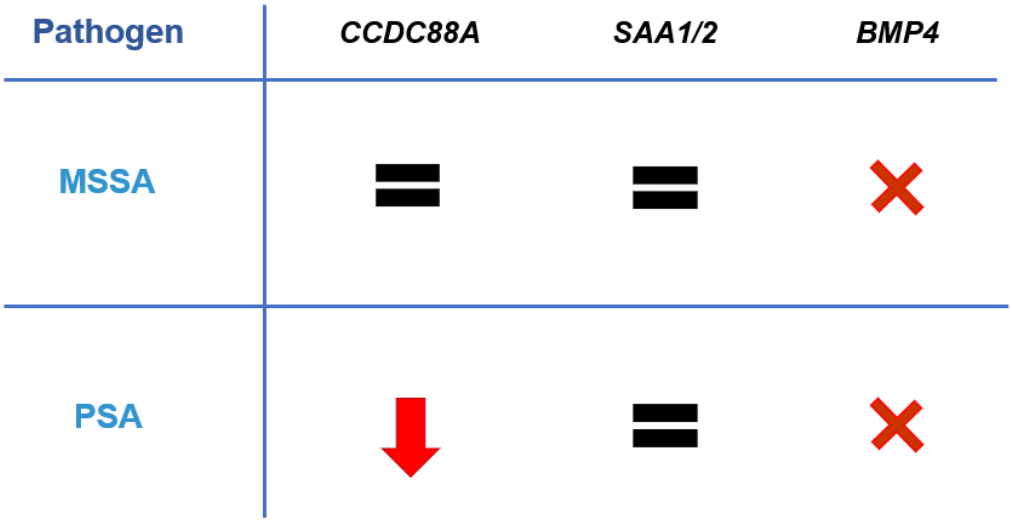

Scheme 2 –Summary schematic representation of the results. (A) Potential biomarkers of bone health and their presence in the different CF patient groups. (B) *CCDC88A*, *SAA1/2* and *BMP4* expression in THP-1 derived macrophages after infection with methicillin-susceptible *S. aureus* (MSSA) or *Pseudomonas aeruginosa* (PSA).

References

1. Andersen, D.H., *Cystic fibrosis of the pancreas and its relation to celiac disease: A clinical and pathologic study.* Am. J. Dis. Child, 1938: p. 344–399.
2. Shteinberg, M., et al., *Cystic fibrosis.* Lancet, 2021. **397**(10290): p. 2195-2211.
3. Guo, X., et al., *Clinical and genetic characteristics of cystic fibrosis in CHINESE patients: a systemic review of reported cases.* Orphanet J Rare Dis, 2018. **13**(1): p. 224.
4. Stewart, C. and M.S. Pepper, *Cystic fibrosis on the African continent.* Genet Med, 2016. **18**(7): p. 653-62.
5. Fonseca, O., et al., *Cystic Fibrosis Bone Disease: The Interplay between CFTR Dysfunction and Chronic Inflammation.* Biomolecules, 2023. **13**(3).
6. *Cystic Fibrosis Foundation Patient Registry 2022 Annual Data Report*. 2022, Cystic Fibrosis Foundation.
7. Plant, B.J., et al., *Management of comorbidities in older patients with cystic fibrosis.* Lancet Respir Med, 2013. **1**(2): p. 164-74.
8. *2023 Cystic Fibrosis Foundation Patient Registry Highlights Handout*, C.F. Foundation, Editor. 2023.
9. Cutting, G.R., *Cystic fibrosis genetics: from molecular understanding to clinical application.* Nat Rev Genet, 2015. **16**(1): p. 45-56.
10. Anderson, M.P., et al., *Demonstration that CFTR is a chloride channel by alteration of its anion selectivity.* Science, 1991. **253**(5016): p. 202-5.
11. Liu, F., et al., *Molecular Structure of the Human CFTR Ion Channel.* Cell, 2017. **169**(1): p. 85-95.e8.
12. Boucher, R.C., *New concepts of the pathogenesis of cystic fibrosis lung disease.* Eur Respir J, 2004. **23**(1): p. 146-58.
13. Brennan, S., et al., *Alveolar macrophages and CC chemokines are increased in children with cystic fibrosis.* Eur Respir J, 2009. **34**(3): p. 655-61.
14. Douglas, T.A., et al., *Acquisition and eradication of P. aeruginosa in young children with cystic fibrosis.* Eur Respir J, 2009. **33**(2): p. 305-11.
15. Lévêque, M., et al., *The impact of impaired macrophage functions in cystic fibrosis disease progression.* J Cyst Fibros, 2017. **16**(4): p. 443-453.
16. Jia, S. and J.L. Taylor-Cousar, *Cystic Fibrosis Modulator Therapies.* Annu Rev Med, 2023. **74**: p. 413-426.
17. Veit, G., et al., *From CFTR biology toward combinatorial pharmacotherapy: expanded classification of cystic fibrosis mutations.* Mol Biol Cell, 2016. **27**(3): p. 424-33.
18. Du, K. and G.L. Lukacs, *Cooperative assembly and misfolding of CFTR domains in vivo.* Mol Biol Cell, 2009. **20**(7): p. 1903-15.
19. Mendoza, J.L., et al., *Requirements for efficient correction of ΔF508 CFTR revealed by analyses of evolved sequences.* Cell, 2012. **148**(1-2): p. 164-74.
20. Rabeh, W.M., et al., *Correction of both NBD1 energetics and domain interface is required to restore ΔF508 CFTR folding and function.* Cell, 2012. **148**(1-2): p. 150-63.
21. Chevalier, B. and A. Hinzpeter, *The influence of CFTR complex alleles on precision therapy of cystic fibrosis.* J Cyst Fibros, 2020. **19 Suppl 1**: p. S15-s18.
22. Sosnay, P.R., et al., *Defining the disease liability of variants in the cystic fibrosis transmembrane conductance regulator gene.* Nat Genet, 2013. **45**(10): p. 1160-7.
23. Costa, E., et al., *The impact of FDA and EMA regulatory decision-making process on the access to CFTR modulators for the treatment of cystic fibrosis.* Orphanet J Rare Dis, 2022. **17**(1): p. 188.

24. Adams, M.A., *Fuctional anatomy of the musculoskeletal system*, in *Gray's Anatomy: The Anatomical Basisof Clinical Practice*, S. Standring and C.B. Wigley, Editors. 2016, Elsevier: Amsterdam, The Netherlands. p. 84–96.
25. Feng, X. and J.M. McDonald, *Disorders of bone remodeling.* Annu Rev Pathol, 2011. **6**: p. 121-45.
26. Clarke, B., *Normal bone anatomy and physiology.* Clin J Am Soc Nephrol, 2008. **3 Suppl 3**(Suppl 3): p. S131-9.
27. Zhou, B.O., et al., *Leptin-receptor-expressing mesenchymal stromal cells represent the main source of bone formed by adult bone marrow.* Cell Stem Cell, 2014. **15**(2): p. 154-68.
28. Park, D., et al., *Endogenous bone marrow MSCs are dynamic, fate-restricted participants in bone maintenance and regeneration.* Cell Stem Cell, 2012. **10**(3): p. 259-72.
29. Oliveira, T.C., M.S. Gomes, and A.C. Gomes, *The Crossroads between Infection and Bone Loss.* Microorganisms, 2020. **8**(11).
30. Hasegawa, T., J. Kikuta, and M. Ishii, *Imaging the Bone-Immune Cell Interaction in Bone Destruction.* Front Immunol, 2019. **10**: p. 596.
31. Li, H., et al., *Osteoporosis: Mechanism, Molecular Target and Current Status on Drug Development.* Curr Med Chem, 2021. **28**(8): p. 1489-1507.
32. Anabtawi, A., et al., *Trabecular bone score in people with cystic fibrosis.* Osteoporos Int, 2022. **33**(5): p. 1137-1145.
33. Aris, R.M., et al., *Increased rate of fractures and severe kyphosis: sequelae of living into adulthood with cystic fibrosis.* Ann Intern Med, 1998. **128**(3): p. 186-93.
34. Mathiesen, I.H., et al., *Osteoporosis Is Associated with Deteriorating Clinical Status in Adults with Cystic Fibrosis.* Int J Endocrinol, 2018. **2018**: p. 4803974.
35. Mailhot, G., et al., *Impaired rib bone mass and quality in end-stage cystic fibrosis patients.* Bone, 2017. **98**: p. 9-17.
36. Latzin, P., et al., *Sternal fracture with fatal outcome in cystic fibrosis.* Thorax, 2005. **60**(7): p. 616.
37. Mora Vallellano, J., et al., *Evaluation of bone metabolism in children with cystic fibrosis.* Bone, 2021. **147**: p. 115929.
38. Dif, F., et al., *Severe osteopenia in CFTR-null mice.* Bone, 2004. **35**(3): p. 595-603.
39. Pashuck, T.D., et al., *Murine model for cystic fibrosis bone disease demonstrates osteopenia and sex-related differences in bone formation.* Pediatr Res, 2009. **65**(3): p. 311-6.
40. Le Henaff, C., et al., *The F508del mutation in cystic fibrosis transmembrane conductance regulator gene impacts bone formation.* Am J Pathol, 2012. **180**(5): p. 2068-75.
41. Haston, C.K., et al., *Persistent osteopenia in adult cystic fibrosis transmembrane conductance regulator-deficient mice.* Am J Respir Crit Care Med, 2008. **177**(3): p. 309-15.
42. Haworth, C.S., et al., *Bone histomorphometry in adult patients with cystic fibrosis.* Chest, 2000. **118**(2): p. 434-9.
43. Braun, C., et al., *Children and adolescents with cystic fibrosis display moderate bone microarchitecture abnormalities: data from high-resolution peripheral quantitative computed tomography.* Osteoporos Int, 2017. **28**(11): p. 3179-3188.
44. King, S.J., et al., *Reduced bone density in cystic fibrosis: DeltaF508 mutation is an independent risk factor.* Eur Respir J, 2005. **25**(1): p. 54-61.
45. Velard, F., et al., *Cystic fibrosis and bone disease: defective osteoblast maturation with the F508del mutation in cystic fibrosis transmembrane conductance regulator.* Am J Respir Crit Care Med, 2014. **189**(6): p. 746-8.
46. Gimenez-Maitre, A., et al., *Deficit of osteoprotegerin release by osteoblasts from a patient with cystic fibrosis.* Eur Respir J, 2012. **39**(3): p. 780-1.

47. Le Henaff, C., et al., *Increased NF-κB Activity and Decreased Wnt/β-Catenin Signaling Mediate Reduced Osteoblast Differentiation and Function in ΔF508 Cystic Fibrosis Transmembrane Conductance Regulator (CFTR) Mice.* J Biol Chem, 2015. **290**(29): p. 18009-18017.
48. Le Heron, L., et al., *Cystic fibrosis transmembrane conductance regulator (CFTR) regulates the production of osteoprotegerin (OPG) and prostaglandin (PG) E2 in human bone.* J Cyst Fibros, 2010. **9**(1): p. 69-72.
49. Lam, G.Y., et al., *IL-8 correlates with reduced baseline femoral neck bone mineral density in adults with cystic fibrosis: a single center retrospective study.* Sci Rep, 2021. **11**(1): p. 15405.
50. Delion, M., et al., *Overexpression of RANKL in osteoblasts: a possible mechanism of susceptibility to bone disease in cystic fibrosis.* J Pathol, 2016. **240**(1): p. 50-60.
51. Tarique, A.A., et al., *Differential expression of genes and receptors in monocytes from patients with cystic fibrosis.* J Cyst Fibros, 2019. **18**(3): p. 342-348.
52. Putman, M.S., et al., *The Effects of Ivacaftor on Bone Density and Microarchitecture in Children and Adults with Cystic Fibrosis.* J Clin Endocrinol Metab, 2021. **106**(3): p. e1248-e1261.
53. Sermet-Gaudelus, I., et al., *Bone demineralization is improved by ivacaftor in patients with cystic fibrosis carrying the p.Gly551Asp mutation.* J Cyst Fibros, 2016. **15**(6): p. e67-e69.
54. Le Henaff, C., et al., *Enhanced F508del-CFTR channel activity ameliorates bone pathology in murine cystic fibrosis.* Am J Pathol, 2014. **184**(4): p. 1132-1141.
55. Briaud, P., et al., *Impact of Coexistence Phenotype Between Staphylococcus aureus and Pseudomonas aeruginosa Isolates on Clinical Outcomes Among Cystic Fibrosis Patients.* Front Cell Infect Microbiol, 2020. **10**: p. 266.
56. Mogayzel, P.J., Jr., et al., *Cystic Fibrosis Foundation pulmonary guideline. pharmacologic approaches to prevention and eradication of initial Pseudomonas aeruginosa infection.* Ann Am Thorac Soc, 2014. **11**(10): p. 1640-50.
57. Reynolds, D. and M. Kollef, *The Epidemiology and Pathogenesis and Treatment of Pseudomonas aeruginosa Infections: An Update.* Drugs, 2021. **81**(18): p. 2117-2131.
58. Jolly, A.L., et al., *Pseudomonas aeruginosa-induced bleb-niche formation in epithelial cells is independent of actinomyosin contraction and enhanced by loss of cystic fibrosis transmembrane-conductance regulator osmoregulatory function.* mBio, 2015. **6**(2): p. e02533.
59. Goss, C.H. and M.S. Muhlebach, *Review: Staphylococcus aureus and MRSA in cystic fibrosis.* J Cyst Fibros, 2011. **10**(5): p. 298-306.
60. Li, Z., et al., *Longitudinal development of mucoid Pseudomonas aeruginosa infection and lung disease progression in children with cystic fibrosis.* Jama, 2005. **293**(5): p. 581-8.
61. Bruscia, E.M. and T.L. Bonfield, *Update on Innate and Adaptive Immunity in Cystic Fibrosis.* Clin Chest Med, 2022. **43**(4): p. 603-615.
62. Bhagirath, A.Y., et al., *Cystic fibrosis lung environment and Pseudomonas aeruginosa infection.* BMC Pulm Med, 2016. **16**(1): p. 174.
63. Li, C., et al., *Staphylococcus aureus Survives in Cystic Fibrosis Macrophages, Forming a Reservoir for Chronic Pneumonia.* Infect Immun, 2017. **85**(5).
64. Averna, M., P. Melotti, and C. Sorio, *Revisiting the Role of Leukocytes in Cystic Fibrosis.* Cells, 2021. **10**(12).
65. Malhotra, S., D. Hayes, Jr., and D.J. Wozniak, *Mucoid Pseudomonas aeruginosa and regional inflammation in the cystic fibrosis lung.* J Cyst Fibros, 2019. **18**(6): p. 796-803.
66. Shmarina, G., et al., *TNF gene polymorphisms in cystic fibrosis patients: contribution to the disease progression.* J Transl Med, 2013. **11**: p. 19.

67. Li, Y., et al., *Endogenous TNFalpha lowers maximum peak bone mass and inhibits osteoblastic Smad activation through NF-kappaB.* J Bone Miner Res, 2007. **22**(5): p. 646-55.
68. Haworth, C.S., et al., *Inflammatory related changes in bone mineral content in adults with cystic fibrosis.* Thorax, 2004. **59**(7): p. 613-7.
69. Aris, R.M., et al., *Adverse alterations in bone metabolism are associated with lung infection in adults with cystic fibrosis.* Am J Respir Crit Care Med, 2000. **162**(5): p. 1674-8.
70. Osta, B., G. Benedetti, and P. Miossec, *Classical and Paradoxical Effects of TNF-α on Bone Homeostasis.* Front Immunol, 2014. **5**: p. 48.
71. Yeh, J.J., et al., *Association of Respiratory Tuberculosis with Incident Bone Fracture: Bridging the Tuberculosis Airway Infection and the Osteoporotic Bone.* PLoS One, 2016. **11**(12): p. e0168673.
72. Gomes, A.C., et al., *Serum amyloid A proteins reduce bone mass during mycobacterial infections.* Front Immunol, 2023. **14**: p. 1168607.
73. Aris, R.M., et al., *Guide to bone health and disease in cystic fibrosis.* J Clin Endocrinol Metab, 2005. **90**(3): p. 1888-96.
74. Marquette, M. and C.S. Haworth, *Bone health and disease in cystic fibrosis.* Paediatr Respir Rev, 2016. **20 Suppl**: p. 2-5.
75. Thaler, R., et al., *Acute-phase protein serum amyloid A3 is a novel paracrine coupling factor that controls bone homeostasis.* Faseb j, 2015. **29**(4): p. 1344-59.
76. Aslam, B., et al., *Proteomics: Technologies and Their Applications.* Journal of Chromatographic Science, 2017. **55**(2): p. 182-196.
77. Roxo-Rosa, M., et al., *Proteomics techniques for cystic fibrosis research.* J Cyst Fibros, 2004. **3 Suppl 2**: p. 85-9.
78. Roxo-Rosa, M., et al., *Proteomic analysis of nasal cells from cystic fibrosis patients and non-cystic fibrosis control individuals: search for novel biomarkers of cystic fibrosis lung disease.* Proteomics, 2006. **6**(7): p. 2314-25.
79. Sloane, A.J., et al., *Proteomic analysis of sputum from adults and children with cystic fibrosis and from control subjects.* Am J Respir Crit Care Med, 2005. **172**(11): p. 1416-26.
80. Liessi, N., et al., *Proteomics and Metabolomics for Cystic Fibrosis Research.* Int J Mol Sci, 2020. **21**(15).
81. Frischer, T., et al., *Possible dysregulation of chaperon and metabolic proteins in cystic fibrosis bronchial tissue.* Proteomics, 2006. **6**(11): p. 3381-8.
82. Gharib, S.A., et al., *Mapping the lung proteome in cystic fibrosis.* J Proteome Res, 2009. **8**(6): p. 3020-8.
83. Dong, K., et al., *Identification of novel blood biomarkers of treatment response in cystic fibrosis pulmonary exacerbations by label-free quantitative proteomics.* Sci Rep, 2019. **9**(1): p. 17126.
84. Debyser, G., et al., *Faecal proteomics: A tool to investigate dysbiosis and inflammation in patients with cystic fibrosis.* J Cyst Fibros, 2016. **15**(2): p. 242-50.
85. Zhang, Y., et al., *Protein analysis by shotgun/bottom-up proteomics.* Chem Rev, 2013. **113**(4): p. 2343-94.
86. Shuken, S.R., *An Introduction to Mass Spectrometry-Based Proteomics.* J Proteome Res, 2023. **22**(7): p. 2151-2171.
87. Ullal, J., et al., *Treatment of cystic fibrosis related bone disease.* J Clin Transl Endocrinol, 2022. **27**: p. 100291.
88. Sermet-Gaudelus, I., et al., *European cystic fibrosis bone mineralisation guidelines.* J Cyst Fibros, 2011. **10 Suppl 2**: p. S16-23.
89. Atlas, G., et al., *The clinical features that contribute to poor bone health in young Australians living with cystic fibrosis: A recommendation for BMD screening.* Pediatr Pulmonol, 2021. **56**(7): p. 2014-2022.

90. Ratti, G.A., et al., *Bone mineral density screening by DXA for people with cystic fibrosis: A registry analysis of patient and program factors influencing rates of screening.* J Cyst Fibros, 2022. **21**(5): p. 784-791.
91. Foundation, C.F., *C.F.P. 2020 Annual Data Report*. 2021.
92. Gensburger, D., et al., *Reduced bone volumetric density and weak correlation between infection and bone markers in cystic fibrosis adult patients.* Osteoporos Int, 2016. **27**(9): p. 2803-2813.
93. Mathiesen, I.H., et al., *Markers of bone turnover are reduced in patients with CF related diabetes; the role of glucose.* J Cyst Fibros, 2019. **18**(3): p. 436-441.
94. Putman, M.S., et al., *Compromised bone microarchitecture and estimated bone strength in young adults with cystic fibrosis.* J Clin Endocrinol Metab, 2014. **99**(9): p. 3399-407.
95. Silva Júnior, C.C.D., et al., *Evaluation of anthropometry as an alternative to DXA as predictor of low bone mineral density in children and adolescents with cystic fibrosis.* Clin Nutr ESPEN, 2021. **45**: p. 229-235.
96. Osório, H., et al., *Proteomics Analysis of Gastric Cancer Patients with Diabetes Mellitus.* J Clin Med, 2021. **10**(3).
97. Liao, Y., et al., *WebGestalt 2019: gene set analysis toolkit with revamped UIs and APIs.* Nucleic Acids Res, 2019. **47**(W1): p. W199-w205.
98. Carey, J.J. and M.F. Delaney, *T-Scores and Z-Scores.* Clinical Reviews in Bone and Mineral Metabolism, 2010. **8**: p. 113–121.
99. Benabdelkamel, H., et al., *Serum-Based Proteomics Profiling in Adult Patients with Cystic Fibrosis.* Int J Mol Sci, 2020. **21**(19).
100. Lepissier, A., et al., *Inflammation biomarkers in sputum for clinical trials in cystic fibrosis: current understanding and gaps in knowledge.* J Cyst Fibros, 2022. **21**(4): p. 691-706.
101. Bene, Z., et al., *Laboratory biomarkers for lung disease severity and progression in cystic fibrosis.* Clin Chim Acta, 2020. **508**: p. 277-286.
102. Muhlebach, M.S., et al., *Biomarkers for cystic fibrosis drug development.* J Cyst Fibros, 2016. **15**(6): p. 714-723.
103. Maher, R.E., et al., *The relationship between lung disease severity and the sputum proteome in cystic fibrosis.* Respir Med, 2022. **204**: p. 107002.
104. Charro, N., et al., *Serum proteomics signature of cystic fibrosis patients: a complementary 2-DE and LC-MS/MS approach.* J Proteomics, 2011. **74**(1): p. 110-26.
105. Rauniyar, N., et al., *Quantitative proteomic profiling reveals differentially regulated proteins in cystic fibrosis cells.* J Proteome Res, 2014. **13**(11): p. 4668-75.
106. Braccia, C., et al., *SWATH label-free proteomics for cystic fibrosis research.* J Cyst Fibros, 2019. **18**(4): p. 501-506.
107. Lartey, J., et al., *Altered Expression of Human Smooth Muscle Myosin Phosphatase Targeting (MYPT) Isovariants with Pregnancy and Labor.* PLoS One, 2016. **11**(10): p. e0164352.
108. Teichgräber, V., et al., *Ceramide accumulation mediates inflammation, cell death and infection susceptibility in cystic fibrosis.* Nat Med, 2008. **14**(4): p. 382-91.
109. Soleti, R., C. Porro, and M.C. Martínez, *Apoptotic process in cystic fibrosis cells.* Apoptosis, 2013. **18**(9): p. 1029-38.
110. Roesch, E.A., D.P. Nichols, and J.F. Chmiel, *Inflammation in cystic fibrosis: An update.* Pediatr Pulmonol, 2018. **53**(S3): p. S30-s50.
111. Craze, M.L., et al., *Glutamate dehydrogenase (GLUD1) expression in breast cancer.* Breast Cancer Res Treat, 2019. **174**(1): p. 79-91.
112. Pollard, P.J., N.C. Wortham, and I.P. Tomlinson, *The TCA cycle and tumorigenesis: the examples of fumarate hydratase and succinate dehydrogenase.* Ann Med, 2003. **35**(8): p. 632-9.

113. Favia, M., et al., *An Intriguing Involvement of Mitochondria in Cystic Fibrosis.* J Clin Med, 2019. **8**(11).
114. Liang, L., et al., *Genetic analysis of acute intermittent porphyria caused by novel classical splicing variant in the insertion region of 29-residue specific to human HMBS protein.* Front Mol Biosci, 2023. **10**: p. 1230798.
115. Vanakker, O.M., M.J. Hosen, and A.D. Paepe, *The ABCC6 transporter: what lessons can be learnt from other ATP-binding cassette transporters?* Front Genet, 2013. **4**: p. 203.
116. Moliteo, E., et al., *Cystic Fibrosis and Oxidative Stress: The Role of CFTR.* Molecules, 2022. **27**(16).
117. Hall, A., *Rho family GTPases.* Biochem Soc Trans, 2012. **40**(6): p. 1378-82.
118. Billuart, P., et al., *Oligophrenin-1 encodes a rhoGAP protein involved in X-linked mental retardation.* Nature, 1998. **392**(6679): p. 923-6.
119. Harrell Stewart, D.R. and G.J. Clark, *Pumping the brakes on RAS - negative regulators and death effectors of RAS.* J Cell Sci, 2020. **133**(3).
120. Campa, F., et al., *A PH domain in the Arf GTPase-activating protein (GAP) ARAP1 binds phosphatidylinositol 3,4,5-trisphosphate and regulates Arf GAP activity independently of recruitment to the plasma membranes.* J Biol Chem, 2009. **284**(41): p. 28069-28083.
121. Weivoda, M.M. and M.J. Oursler, *The Roles of Small GTPases in Osteoclast Biology.* Orthop Muscular Syst, 2014. **3**.
122. Itzstein, C., F.P. Coxon, and M.J. Rogers, *The regulation of osteoclast function and bone resorption by small GTPases.* Small GTPases, 2011. **2**(3): p. 117-130.
123. Mariño, G., et al., *Premature aging in mice activates a systemic metabolic response involving autophagy induction.* Human Molecular Genetics, 2008. **17**(14): p. 2196-2211.
124. Mariño, G., et al., *Insulin-like growth factor 1 treatment extends longevity in a mouse model of human premature aging by restoring somatotroph axis function.* Proc Natl Acad Sci U S A, 2010. **107**(37): p. 16268-73.
125. Olney, R.C., *Regulation of bone mass by growth hormone.* Med Pediatr Oncol, 2003. **41**(3): p. 228-34.
126. Höög, J.O., et al., *The mammalian alcohol dehydrogenases interact in several metabolic pathways.* Chem Biol Interact, 2003. **143-144**: p. 175-81.
127. Maléth, J., et al., *Alcohol disrupts levels and function of the cystic fibrosis transmembrane conductance regulator to promote development of pancreatitis.* Gastroenterology, 2015. **148**(2): p. 427-39.e16.
128. Ferdinandusse, S., et al., *Identification of the peroxisomal beta-oxidation enzymes involved in the biosynthesis of docosahexaenoic acid.* J Lipid Res, 2001. **42**(12): p. 1987-95.
129. Kleme, M.L. and E. Levy, *Cystic fibrosis-related oxidative stress and intestinal lipid disorders.* Antioxid Redox Signal, 2015. **22**(7): p. 614-31.
130. Lépine, J., et al., *Specificity and regioselectivity of the conjugation of estradiol, estrone, and their catecholestrogen and methoxyestrogen metabolites by human uridine diphospho-glucuronosyltransferases expressed in endometrium.* J Clin Endocrinol Metab, 2004. **89**(10): p. 5222-32.
131. Wasmuth, H.E., et al., *Coinheritance of Gilbert syndrome-associated UGT1A1 mutation increases gallstone risk in cystic fibrosis.* Hepatology, 2006. **43**(4): p. 738-41.
132. Désiré, J., et al., *N- and C-alkylation of seven-membered iminosugars generates potent glucocerebrosidase inhibitors and F508del-CFTR correctors.* Org Biomol Chem, 2014. **12**(44): p. 8977-96.
133. Dechecchi, M.C., et al., *Anti-inflammatory effect of miglustat in bronchial epithelial cells.* J Cyst Fibros, 2008. **7**(6): p. 555-65.

134. Hu, Q., et al., *CCDC88A Post-Transcriptionally Regulates VEGF via miR-101 and Subsequently Regulates Hepatocellular Carcinoma.* Front Immunol, 2022. **13**: p. 859331.
135. Bouzat, C., et al., *Molecular function of α7 nicotinic receptors as drug targets.* J Physiol, 2018. **596**(10): p. 1847-1861.
136. Weng, L., et al., *Girding for migratory cues: roles of the Akt substrate Girdin in cancer progression and angiogenesis.* Cancer Sci, 2010. **101**(4): p. 836-42.
137. Ghosh, P., et al., *Biochemical, Biophysical and Cellular Techniques to Study the Guanine Nucleotide Exchange Factor, GIV/Girdin.* Curr Protoc Chem Biol, 2016. **8**(4): p. 265-298.
138. Wang, X., et al., *CCDC88A/GIV promotes HBV replication and progeny secretion via enhancing endosomal trafficking and blocking autophagic degradation.* Autophagy, 2022. **18**(2): p. 357-374.
139. Wang, H., et al., *GIV/girdin links vascular endothelial growth factor signaling to Akt survival signaling in podocytes independent of nephrin.* J Am Soc Nephrol, 2015. **26**(2): p. 314-27.
140. Liang, B., et al., *Dimethyloxaloylglycine-stimulated human bone marrow mesenchymal stem cell-derived exosomes enhance bone regeneration through angiogenesis by targeting the AKT/mTOR pathway.* Stem Cell Res Ther, 2019. **10**(1): p. 335.
141. Chen, J. and F. Long, *mTOR signaling in skeletal development and disease.* Bone Res, 2018. **6**: p. 1.
142. Sack, G.H., Jr., *Serum amyloid A - a review.* Mol Med, 2018. **24**(1): p. 46.
143. Choudhary, S., et al., *Serum Amyloid A3 Secreted by Preosteoclasts Inhibits Parathyroid Hormone-stimulated cAMP Signaling in Murine Osteoblasts.* J Biol Chem, 2016. **291**(8): p. 3882-94.
144. Ribeiro, C.M.P. and M. Gentzsch, *Impact of Airway Inflammation on the Efficacy of CFTR Modulators.* Cells, 2021. **10**(11).
145. Rehman, T., et al., *Inflammatory cytokines TNF-α and IL-17 enhance the efficacy of cystic fibrosis transmembrane conductance regulator modulators.* J Clin Invest, 2021. **131**(16).
146. Shteinberg, M. and J.L. Taylor-Cousar, *Impact of CFTR modulator use on outcomes in people with severe cystic fibrosis lung disease.* Eur Respir Rev, 2020. **29**(155).
147. Li, W., et al., *Induction of pro-inflammatory genes by serum amyloid A1 in human amnion fibroblasts.* Sci Rep, 2017. **7**(1): p. 693.
148. Jumeau, C., et al., *Expression of SAA1, SAA2 and SAA4 genes in human primary monocytes and monocyte-derived macrophages.* PLoS One, 2019. **14**(5): p. e0217005.
149. De Buck, M., et al., *The cytokine-serum amyloid A-chemokine network.* Cytokine Growth Factor Rev, 2016. **30**: p. 55-69.
150. Miyazono, K., S. Maeda, and T. Imamura, *BMP receptor signaling: transcriptional targets, regulation of signals, and signaling cross-talk.* Cytokine Growth Factor Rev, 2005. **16**(3): p. 251-63.
151. Chen, Y., et al., *Potential Functions of the BMP Family in Bone, Obesity, and Glucose Metabolism.* J Diabetes Res, 2021. **2021**: p. 6707464.
152. Lee, Y.C., et al., *BMP4 promotes prostate tumor growth in bone through osteogenesis.* Cancer Res, 2011. **71**(15): p. 5194-203.
153. Gozo, M.C., et al., *Foxc2 induces Wnt4 and Bmp4 expression during muscle regeneration and osteogenesis.* Cell Death Differ, 2013. **20**(8): p. 1031-42.
154. Bordukalo-Nikšić, T., V. Kufner, and S. Vukičević, *The Role Of BMPs in the Regulation of Osteoclasts Resorption and Bone Remodeling: From Experimental Models to Clinical Applications.* Front Immunol, 2022. **13**: p. 869422.

155. Bandyopadhyay, A., et al., *Genetic analysis of the roles of BMP2, BMP4, and BMP7 in limb patterning and skeletogenesis.* PLoS Genet, 2006. **2**(12): p. e216.
156. Schlickewei, C., et al., *A bioactive nano-calcium phosphate paste for in-situ transfection of BMP-7 and VEGF-A in a rabbit critical-size bone defect: results of an in vivo study.* Journal of Materials Science: Materials in Medicine, 2019. **30**: p. 1-12.
157. Huang, X.Y., et al., *Directed osteogenic differentiation of human bone marrow mesenchymal stem cells via sustained release of BMP4 from PBVHx-based nanoparticles.* Int J Biol Macromol, 2024. **265**(Pt 1): p. 130649.
158. Reilly, R., et al., *Targeting the PI3K/Akt/mTOR signalling pathway in Cystic Fibrosis.* Sci Rep, 2017. **7**(1): p. 7642.
159. Pulito, C., et al., *Metformin-induced ablation of microRNA 21-5p releases Sestrin-1 and CAB39L antitumoral activities.* Cell Discov, 2017. **3**: p. 17022.
160. He, J., et al., *Polyphyllin I induces autophagy and cell cycle arrest via inhibiting PDK1/Akt/mTOR signal and downregulating cyclin B1 in human gastric carcinoma HGC-27 cells.* Biomed Pharmacother, 2019. **117**: p. 109189.
161. Tan, J., et al., *PDK1 signaling toward PLK1-MYC activation confers oncogenic transformation, tumor-initiating cell activation, and resistance to mTOR-targeted therapy.* Cancer Discov, 2013. **3**(10): p. 1156-71.
162. Liu, J., et al., *Protein phosphatase PPM1G regulates protein translation and cell growth by dephosphorylating 4E binding protein 1 (4E-BP1).* J Biol Chem, 2013. **288**(32): p. 23225-33.
163. Mercier, J., et al., *SLC6A14 Impacts Cystic Fibrosis Lung Disease Severity via mTOR and Epithelial Repair Modulation.* Front Mol Biosci, 2022. **9**: p. 850261.
164. Tsuchiya, M., et al., *RPTOR, a novel target of miR-155, elicits a fibrotic phenotype of cystic fibrosis lung epithelium by upregulating CTGF.* RNA Biol, 2016. **13**(9): p. 837-47.
165. Xia, D., et al., *MARCH2 regulates autophagy by promoting CFTR ubiquitination and degradation and PIK3CA-AKT-MTOR signaling.* Autophagy, 2016. **12**(9): p. 1614-30.
166. Woodworth, B.A., et al., *The delta F508 mutation in cystic fibrosis and impact on sinus development.* Am J Rhinol, 2007. **21**(1): p. 122-7.
167. Elkin, S.L., et al., *Vertebral deformities and low bone mineral density in adults with cystic fibrosis: a cross-sectional study.* Osteoporos Int, 2001. **12**(5): p. 366-72.
168. Szczesniak, R., et al., *Use of FEV(1) in cystic fibrosis epidemiologic studies and clinical trials: A statistical perspective for the clinical researcher.* J Cyst Fibros, 2017. **16**(3): p. 318-326.
169. Mou, H., et al., *Generation of multipotent lung and airway progenitors from mouse ESCs and patient-specific cystic fibrosis iPSCs.* Cell Stem Cell, 2012. **10**(4): p. 385-97.
170. Lee, H., et al., *mTORC1 is a mechanosensor that regulates surfactant function and lung compliance during ventilator-induced lung injury.* JCI Insight, 2021. **6**(14).
171. Houssaini, A., et al., *mTOR pathway activation drives lung cell senescence and emphysema.* JCI Insight, 2018. **3**(3).
172. Liu, T., et al., *Optimization of differentiation and transcriptomic profile of THP-1 cells into macrophage by PMA.* PLoS One, 2023. **18**(7): p. e0286056.
173. Deng, Q., et al., *Pseudomonas aeruginosa Triggers Macrophage Autophagy To Escape Intracellular Killing by Activation of the NLRP3 Inflammasome.* Infect Immun, 2016. **84**(1): p. 56-66.
174. Dal Negro, R.W., et al., *A two-stage logistic model based on the measurement of pro-inflammatory cytokines in bronchial secretions for assessing bacterial, viral, and non-infectious origin of COPD exacerbations.* Copd, 2005. **2**(1): p. 7-16.

175. Aufiero, B., et al., *Staphylococcus aureus induces the expression of tumor necrosis factor-alpha in primary human keratinocytes.* Int J Dermatol, 2007. **46**(7): p. 687-94.
176. Rahman, M.M. and G. McFadden, *Modulation of tumor necrosis factor by microbial pathogens.* PLoS Pathog, 2006. **2**(2): p. e4.
177. Nakase, T., et al., *Transient and localized expression of bone morphogenetic protein 4 messenger RNA during fracture healing.* J Bone Miner Res, 1994. **9**(5): p. 651-9.
178. Wright, V., et al., *BMP4-expressing muscle-derived stem cells differentiate into osteogenic lineage and improve bone healing in immunocompetent mice.* Mol Ther, 2002. **6**(2): p. 169-78.
179. Wellems, D., et al., *Loss of CFTR function in macrophages alters the cell transcriptional program and delays lung resolution of inflammation.* Front Immunol, 2023. **14**: p. 1242381.
180. Bruscia, E.M., et al., *Macrophages directly contribute to the exaggerated inflammatory response in cystic fibrosis transmembrane conductance regulator-/- mice.* Am J Respir Cell Mol Biol, 2009. **40**(3): p. 295-304.
181. Bonfield, T.L., et al., *Absence of the cystic fibrosis transmembrane regulator (Cftr) from myeloid-derived cells slows resolution of inflammation and infection.* J Leukoc Biol, 2012. **92**(5): p. 1111-22.
182. Covarrubias, A.J., H.I. Aksoylar, and T. Horng, *Control of macrophage metabolism and activation by mTOR and Akt signaling.* Semin Immunol, 2015. **27**(4): p. 286-96.